ELSEVIER

Image and Vision Computing 16 (1998) 473–498

image AND vision COMPUTING

Towards a method for parametrizing models of early vision using psychophysical data

Ela Claridge*, Ian R. Billups

School of Computer Science, The University of Birmingham, Birmingham B15 2TT, UK

Received 1 August 1996; revised 1 July 1997; accepted 23 September 1997

Abstract

Parametrizing computational models of vision, i.e. choosing values for their free parameters, is important both for applied computer vision and for developing the models themselves. A new, principled technique for parametrizing computational models of early vision is presented. It requires that some specific mathematical relationships are found between properties of the input to a model and some suitable psychophysical data. Comparing these either parametrizes the model, allowing it to be implemented as a computer vision system, or refutes it, motivating further modelling. The application of the technique to two computational models of early vision is demonstrated. © 1998 Elsevier Science B.V. All rights reserved.

Keywords: Parametrization; Computational modelling; Early vision

1. Introduction

Vision modelling research has produced many different computational systems, each of which claims to model some part of the human visual system at a particular level of detail. A problem encountered when trying to re-implement these models is that many of them are not fully parametrized, i.e. they include parameters whose values are either unknown or unpublished. Consider, for instance, a very simple system in which a Gaussian filter is applied to a digitized image and which claims to model the blurring effect of lateral retinal interconnections. The size of the Gaussian is the parameter, if it is not given then the model is not parametrized; setting the size of the Gaussian to a particular value parametrizes the model. We argue that parametrization is an important but relatively neglected part of the modelling process and present a method of parametrization which uses psychophysical data.

1.1. Background

The initial stimulus for this work came from an attempt to use a computational model to help to choose between two possible explanations of a psychophysical experiment (see Humphreys et al. [1] 'Qualitative analysis of contour processing 2: Collinearity and contrast polarity'). The model used was Neumann's model [2], based on, but extending, the well-established Grossberg and Mingolla model [3,4]. While carrying out computational experiments we found that the outcome of the model could be substantially changed by small changes in the value of a parameter and that the model's dependence on each of its parameters was itself dependent on the values assigned to all the others. Different parametrizations supported different conclusions and on the basis of these experiments it was impossible to choose between competing explanations. The difficulty of choosing a parametrization for the model thus motivated work towards the development of a principled technique for parametrizing models of early vision, the subject of this paper.

1.2. Information processing models and computational models

Not all models of biological visual systems are meant to be implemented. Some models are conceived to support testing of qualitative nature, which seeks to answer general questions regarding the system's architecture or its information processing model. In Marr's [5] terminology such models are concerned with the computational theories, representations and algorithms. Any parameters present in these models serve to indicate, in general terms, the factors which affect the behaviour of the model. Models of this nature can be collectively called theories. However, if such a theory is to be implemented as a computer program

* Corresponding author.

PII S0262-8856(97)00084-X

(a computational model) and used for simulations, all its parameters have to be given values.

A computational model with free parameters is in fact a *class* of related models. In order to make statements about the relationship between the model and some psychophysical data, or perhaps about the similarity between the behaviour of the model and that of a biological visual system, it is necessary to specify *which* model or class of models is under discussion. If a computational model of a biological visual system is completely parametrized it may be implemented and this implementation may be used to predict the results of psychophysical experiments. Comparison with such results would support or criticize the parametrized model. To evaluate a model itself, it is necessary to find all of its acceptable parametrizations. If a given class of psychophysical results cannot be explained given any of these parametrizations this may indicate that the model is either incomplete or invalid.

Unlike the trivial example of a Gaussian filter given above, a published model may contain many parameters, which may be mutually dependent and interact in complex ways, resulting sometimes in radically different behaviour of the model. If parameter values are not specified, how is the reader to know which of these models is under discussion by the author(s)? If computer simulations are used to support or refute a theory, should a computational model (and its underlying theory) be considered 'valid' if otherwise successful simulations use very different parametrizations for each different stimulus? Even if only general statements are made about the model, they are very unlikely to be true for *all possible* parametrizations.

The practice of publishing model parametrizations is only slowly beginning to take place in vision community [6,7]. This practice, which is common in experimental sciences, is essential for the healthy development of computer vision as a science and it's lack has been criticized in the past. Haralick [8] was one of the first to raise the general issue of "the ad hoc nature of much computer vision research" (p. 385). Since then, awareness of this shortcoming has been increasing in the computer vision community, with papers suggesting general methodologies as well as particular solutions. In the former category Price [9], among the others, vividly makes the point that researchers should share their results and implementations (including parametrization). One of his open questions is particularly relevant in the context of this paper: "How do you control the tuning of algorithms? If the choice of a single threshold can greatly change the entire result, is the solution in the method for choosing the threshold or in the algorithm?". A contribution by Haralick [10] makes similar points. His recent seminal paper 'Performance characterization in computer vision' [11] suggests a general protocol for determining the performance characterization of a vision algorithm. In a related discussion paper, Weng et al. [12] refer specifically to the importance of considering parametrization in characterizing and evaluating the performance of computer vision algorithms.

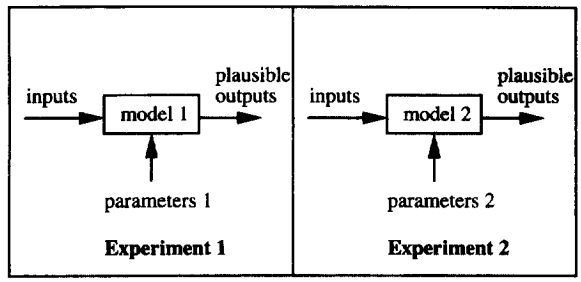

Fig. 1. Two different models (architectures), each using different set of parameters, both produce outputs which are consistent with psychophysical experiments.

1.3. Model parametrization

Any model that has been implemented and used to produce results of simulations must have been completely parametrized. A literature survey (see later) found that the existence of a parametrization technique is usually only *implied* by the existence of a parametrized computational model. Parametrization is rarely mentioned explicitly and very rarely discussed. Where it is, the two most common approaches are either to select parameters by experimentation so that the results of the model fit best the given experimental data[1] or to derive (mathematically) a set of parameters such that the model meets some general criteria (for example, its convergence to a certain state or a solution is guaranteed). Other approaches include the use of neurophysiological measurements (such as for example the size of a receptive field) and their derivatives, or the use of 'learning' techniques, by exposing a model to examples. Although these common themes could be observed, no technique was found whose application to more than one model was discussed, suggesting that no general techniques exist for parametrizing computational models of early vision.[2]

Within the context of our work, the rôle of a computational model was to find support for or to refute a hypothesized information processing model of early vision processes concerned with grouping (see Humphreys et al. [1]). The success criterion was whether or not the model outputs were consistent with the results of psychological experiments, given equivalent stimuli. As the behaviour of parametrized computational models could be made very different, depending on the choice of parameters, the validity of the underlying information processing model could not be established. Two situations occurring commonly in simulations are diagramatically represented in Figs 1 and 2. Fig. 1 illustrates the case where two different models (architectures), each using different set of parameters, both produce outputs which are consistent with psychophysical experiments. Fig. 2 illustrates the case where a given

[1] A model parametrized according to this type of criteria is sometimes referred to as 'isomorphistic'—see Pessoa et al. [6].

[2] The term 'early vision' used here is synonymous with 'pre-attentive vision'.

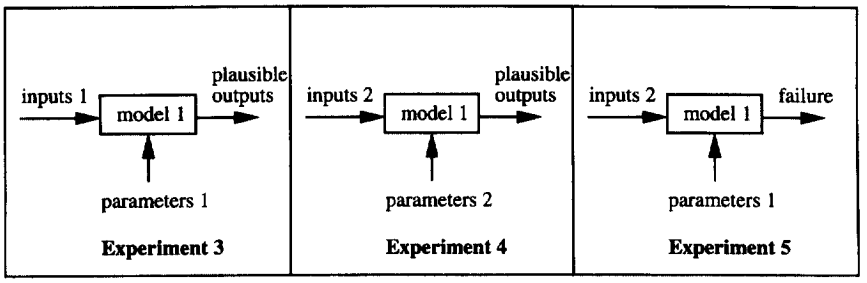

Fig. 2. A given model produced plausible results when different sets of parameters were used for different sets of stimuli; however, the model failed if parameters from experiment 3 were used for the stimulus set in experiment 4.

model produced plausible results when different sets of parameters were used for different sets of stimuli; however, the model failed if parameters from experiment 3 were used for the stimulus set in experiment 4.

Clearly, on the basis of such simulations one cannot draw unambiguous conclusions either about the model itself or about its parameters. The reason is that both the model and the parametrization are the components we are trying to establish. Such a system is undetermined and it is necessary to find some additional criteria; for example, by supplying the system with some 'ground truth' data [13,14]. Psychological experiments can provide a set of inputs and corresponding outputs which characterize the system. If the model and the parametrization are correct then, when presented with the inputs, together they should produce outputs which are consistent with the outputs of psychological experiments. Thus, if we make an assumption that a given architecture is correct and have a set of inputs and outputs, we may be able to recover the parameters. Moreover, if no parameters are found which are consistent with the set of inputs and outputs, this may suggest that the architecture itself is incorrect.

The situation outlined above is reminiscent of a central problem in system theory, namely the recovery of an internal model (a state-variable representation) for a given external model (input–output data). The underlying idea is that the state-variable model provides an *explanation* of the observed data [15]; if model is assumed correct, the variables can be recovered and the internal model made explicit. Our approach to parametrization follows this scheme, in very broad terms. The adopted solutions will be described using system theory concepts, where appropriate.

If $g(\mathbf{k})$, $\mathbf{k} \in K$, indicates an uninstantiated model whose output depends on parameter set $K \subset R^n$, $u(t)$ is an input, t is an instance of a stimulus of the class T and $y(t)$ is the corresponding output, then a simulation can be expressed as:

$$y(t) = g(\mathbf{k}) \otimes u(t). \tag{1}$$

The operator $\otimes$ specifies how g and u are combined (for example, linear combination, convolution, etc.). An evaluation function:

$$\prod : \{y(t)\}_{t \in T} \rightarrow \{0, 1\}, \tag{2}$$

specifies whether the output from a simulation is valid (1) or invalid (0).

Experiments 1 and 2, where the preference for one of two competing models g_1 and g_2 is sought, can be expressed as follows:

$$\exists \mathbf{k}_1, \mathbf{k}_2 \in K \text{ such that } \forall t \in T1$$

$$y(t) = g_1(\mathbf{k}_1) \otimes u(t), \quad \prod(y(t))_{t \in T1} = 1 \text{ and}$$

$$y(t) = g_2(\mathbf{k}_2) \otimes u(t), \quad \prod(y(t))_{t \in T2} = 1. \tag{3}$$

Experiments 3–5, illustrating the use of isomorphistic criteria, can lead to the following situation where the validity of the model g cannot be established:

$$\exists \mathbf{k}_1, \mathbf{k}_2 \in K \text{ such that}$$

$$\forall t \in T1 \; y(t) = g(\mathbf{k}_1) \otimes u(t), \quad \prod(y(t))_{t \in T1} = 1 \text{ and}$$

$$\forall t \in T2 \; y(t) = g(\mathbf{k}_2) \otimes u(t), \quad \prod(y(t))_{t \in T2} = 1 \text{ but}$$

$$\exists t \in T1 \; y(t) = g(\mathbf{k}_2) \otimes u(t), \quad \prod(y(t))_{t \in T1} = 0. \tag{4}$$

1.4. Limitations

It may be helpful to state, at the onset, the limitations to the power and scope of this approach. The early vision system which is the subject of analysis is embedded in a large and complex 'super-system' and it cannot easily be isolated from it. This necessitates making quite strong assumptions regarding the interactions of the sub-system with the super-system. A particularly difficult problem arises from the fact that the outputs from the system are not directly accessible. Our technique has been developed on two assumptions regarding the interactions of the modelled early vision system ('the early vision') and the remaining part of the visual system which receives output from the modelled system and produces output ('the post-processor'). The first assumption is that the entire input on which the output of the system depends is being processed first by the early vision, i.e. no part of the input that has not been processed by the early vision is used to form the output. The second assumption is that the post-processor is consistent. This assumption means that given two identical outputs from the

early vision[3], the post-processor will produce identical outputs.

The usual form of input in vision experiments is an image, which is a very 'non-parametric' representation and is very unlike inputs usually considered in system theory, which can be expressed by a (relatively small) set of parameters. This is also partially true for outputs, although in some experiments the 'output' can be a binary 'yes' or 'no'. One of the novel contributions of this work is a proposal for *parametric* representation for classes of images. A related problem, for which we found a (tentative) solution, is how to express the relationship between the input and output and the system parameters.

One has to carefully consider assumptions made with respect to models underlying experimental data and used to parametrize the system. First, in most such experiments it is assumed that the samples are independent and this cannot be taken for granted in a biological visual system. Second, an assumption originally underlying the contrast sensitivity function (CSF) experiments, used here to parametrize models, was that the visual system's response is a linear combination of outputs of individual frequency-selective channels. If a system or a model is non-linear, then parametrization arrived at on the basis of single-frequency inputs is not guaranteed to be correct for arbitrary inputs.

1.5. Application of the method

The parametrization method is demonstrated in application to two models: Neumann's model [2,16], which is an extension to a well-known Grossberg and Mingolla model, and Watt's [17,18] MIRAGE model. In the first case, it is demonstrated that parametrization can be found, but on the assumption that the model, as described, is a single-frequency model (as, indeed, stated by Neumann). Furthermore, the outcome of parametrization suggests that one of the system parameters considered to be a neurophysiological 'global constant' (the passive decay constant) should in fact take different values for different frequency channels. Taking the 'best' value for this parameter it is shown how two further model parameters (defining the centre-surround architecture) are found. Values of these parameters are within the limits known from neurophysiology. The second demonstration shows that after extending the noise model, estimates can be found for the number of frequency channels and, indirectly, the sizes of the associated spatial filters. Here, the conclusions and the parameters are only tentative because the inclusion of the stochastic component in the model made the parametrization much harder.

[3] But not necessarily two different inputs.

2. Existing techniques

2.1. The scope of the survey

The problem of parametrizing computational models exists in all the sciences, some of the social sciences and in engineering, and so an exhaustive survey of existing techniques would be impractical. As indicated above, parametrization is also one of central problems in system theory. However, because of the problems peculiar to parametrizing models of early vision, it seemed most appropriate to survey the early vision literature which contains non-trivial examples of computer simulations and to identify papers representative of different parametrization methods. The existing, model-specific, techniques for parametrizing computational models of early vision are discussed below. Where a model is chosen to illustrate a particular technique, all the available information about how it was parametrized is presented.

2.2. Unseen techniques

The majority of computational models found are published without any statement of parameter values. Those which are published with parameter values often do not include any indication of how, or why, the values were chosen. Such models are, at least, fully specified and any results shown can be reproduced. Examples include Grossberg and Wyse's [19] and Cohen and Grossberg's [20] models. Another example is the model of Malik and Perona [21], which discriminates regions of different texture in its input directly from the outputs of linear filters, rather than after edge detection. It aims to be general, biologically plausible and to give a quantitative match to psychophysical data about the salience of the boundary between any two textured regions. Parameter values are chosen and the model matches the data as a result, so it is at least implicit why those values were chosen, but not how. A brightness perception model of Pessoa et al. [6] specifies all the parameter values and discusses the rationale for their choices. Gove et al. [22] in their paper on extensions and enhancements to Grossberg's BCS/FCS model, report parameter values for most of the model's parameters; it can be seen that different parameters are often used for different stimuli. This and the previous two papers are examples of 'isomorphistic' models (as referred to by Pessoa et al. [6]) where the parameters are manipulated so that the "output of the model is an activity profile that is, ideally, isomorphistic with a human's brightness distribution in response to the corresponding stimulus".

2.3. Numerical analysis

One example of a principled method for model parametrization is work by Raijmakers et al. [7]. They undertook an interesting study of stability analysis of Exact ART, a

complete implementation of an ART network, which implements on-centre off-surround shunting neural networks using contents-addressable memory. By systematically varying the model parameters σ_e and σ_i (which determine the range of lateral connections) and d_e and d_i (which determine the strength of lateral connections), they employed the numerical bifurcation analysis to study the model's behaviour in this four-dimensional parameter space. The analysis identified several stable regions in the parameter space such that different regions corresponded to different behaviours of the model. Thus, the parameters required for a particular model's outputs could be selected explicitly on the basis of this analysis.

2.4. Neurophysiological techniques

Dobbins et al. [23] presented a computational model of curvature detection that was closely based on the behaviour of end-stopped neurons in the visual cortex of the cat. Their only statement about parametrization was that two of the model's parameters, each analogous to a neuron's receptive field size, were "within physiological limits".

The models of vision proposed by neurophysiologists are clearly based on their knowledge of the structure and function of the biological visual systems they study, e.g. they often propose models with spatial filtering schemes whose behaviour qualitatively resembles that of simple or complex cortical neurons [24]. However, despite the large number of computational models that are physiologically based and that have parameters analogous to neurophysiological values such as receptive field sizes, there are remarkably few examples of such models whose parameter values are set directly from quantitative neurophysiological data. One such example is a model of Heitger et al. [24] in which the ratio of the sizes of two Gaussian filters was set to the ratio of the sizes of two receptive fields, those of neurons in V1 of the monkey cortex and those of neurons in V2, as measured by von der Heydt and Peterhans [25]. It may be that this parametrization technique is used so infrequently because, due to the invasive nature of neurophysiological techniques, quantitative neurophysiological data about the human visual system is scarce.

2.5. Learning techniques

Gerrissen's [26] model of visual search in humans is loosely based on Treisman's [27] feature integration theory and incorporates a multi-layer perceptron network. It is certainly a computational model, although its author calls it an emulation of early vision rather than a simulation, to stress that it is a computer vision application based on a computational model. The weights on the links between its processing units can be considered as a large number of free parameters which are explicitly parametrized when the network is trained (under supervision and by back-propagation of errors). However, it could be argued that this type of model also contains a number of implicit parameters which define its behaviour, for example the overall network architecture, its connectivity structure, the number of neurons and layers, learning rules etc. More interesting, though, is the technique used to parametrize the model of Westland and Foster [29]. Their model combines the outputs of a linear filtering scheme using a non-linear operation, to model detection of oriented line segments. It is similar to Malik and Perona's [21] model of texture discrimination cited above. Its six free parameters were set by simulated annealing: a stochastic technique for solving large optimization problems. In this case, the large optimization problem was to assign values to six parameters so that the model matched some psychophysical data as closely as possible. Simulated annealing can hence be considered as a technique for parametrizing computational models of early vision. Marshall's [28] neural network EXIN is an example of a self-organizing general pattern-recognition system. Its structure (including topology and parameters) develops through the exposure to complex perceptual environments. The in-built basic neural mechanisms (based on neurobiological mechanisms) enable it exhibit phenomena usually associated with 'low-level' vision such as contour completion.

2.6. Psychophysical techniques

While the simulated annealing technique above used psychophysical data to constrain the output of the model, such data may occasionally be used even more directly. Skrzypek and Ringer [30] used a network with competitive feedback to model the perception of anomalous contours. Of the 17 free parameters in the model [31], one was set: the parameter controlling the distance over which the model could form an anomalous contour was set to the largest distance over which the human visual system can form one, as measured by a psychophysical experiment.

Two other models parametrized using psychophysical data are those of Watt [18] and Wilson and Bergen [32]. Watt's [18] model of early vision is based on a set of linear filters whose outputs are combined by a non-linear operation and are not available directly to higher-level visual processes. Watt states values for the parameters controlling the sizes of the smallest and largest of the filters and then goes on to show, using computational simulations, that the model explains the results of three very different psychophysical experiments [17].

The model of Wilson and Bergen [32] had, in fact, been completely parametrized. It is a general model of threshold spatial vision, based on four channels each with different spatial and temporal characteristics. The channels vary in size with retinal eccentricity and their outputs are combined by probability summation to give a measure of the delectability of their input. Parameters were set by constraining the output of the model to match subjects' performance in one detection task and then the completely parametrized

model was used to successfully predict their performance in a different detection task.

2.7. A summary of existing techniques

In summary, only a relatively small number of models of early vision are accompanied by parameter values and by a discussion how these were chosen. The techniques that might be applicable to more than one model, including simulated annealing, the psychophysical techniques and isomorphistic techniques, all used psychophysical data for parametrization. The technique to be proposed in this paper will also use such data.

3. Outline of the parametrization method

As stated in Section 1, to evaluate the model itself it is necessary to find all of its valid parametrizations. A weaker objective is to fully parametrize a model, i.e. to instantiate all its free parameters so that the model's output is valid. Treating both a model and a psychophysical experiment as impulse response functions we consider the output of the model to be valid if it is consistent with the output of a psychophysical experiment, given an equivalent input. A similar approach was adopted by a number of authors [6,21,22]. One important contribution of this paper is to demonstrate a method of parametrization which makes explicit not only what it means for the (output of the) model to be valid but also how the parametrization was arrived at. Psychophysical data is used not only to validate the model, as others do, but also to assign values to model parameters. As such, we consider the method to be principled and thus potentially generally applicable.

At the most abstract level, the method consists of two stages. The first stage is to find suitable input data and to re-describe the model so that the relationship between the output of the model and its input is explicit. Specifically, mathematical analysis is used to express the output of the model (exactly or approximately) as an algebraic formula which incorporates an expression relating the model parameters to the model's input. Ideally this formula should be simple (i.e. should involve only mathematical operations that are familiar and easy to manipulate) and compact (i.e. it should contain relatively few terms when written).

The second stage is to find some experimental data relating the quantity modelled by the output of the model and that modelled by the input and compare them with the model's formula. If the formula is sufficiently simple and compact it should be possible to invert it and thus to find parametrization for the model. If no acceptable parametrization can be found, then the conclusion will be that the model cannot explain the data.

A model can be tested further. For example, it can be parametrized twice, using data from two different psychophysical experiments; ideally, there should be a single parametrization that explains both. In addition, a biologically based model can be parametrized using psychophysical data and then the values of any of its parameters that represent neurophysiological quantities (e.g. sizes of cells' receptive fields) can be compared with appropriate neurophysiological data; ideally, the model should be consistent with both.

3.1. Problems

Applying this method in practice is not straightforward for a number of reasons.

3.1.1. Deriving algebraic formulae

One of the main difficulties is how to re-represent or approximate a model so that it can be expressed as a simple and compact algebraic formula. Models of vision are complex and so are not likely to have simple and compact formulae. They often include awkward operations such as spatial convolution and half-wave rectification. These operations, though well-defined, are hard to manipulate algebraically, so exact formulae for such models will not be simple. The solution we adopted is to use approximations, which are constructed by replacing a part of a formula that was hard to manipulate algebraically with one that is much easier and yet numerically similar (e.g. Segel [33]). Each such approximation is accompanied by an upper bound on the error introduced into the formula. Although clearly necessary for a rigorous analysis, such an upper bound is often hard to find since the error is a function of the part of the formula that was replaced because it was too hard to manipulate. A combination of algebraic and numerical methods is usually needed.

3.1.2. Finding algebraic forms of input

A related problem is finding an analytical (or parametric) form of the input. Models of early vision typically take as input an image (i.e. a two-dimensional array of numbers) which may be represented mathematically as a matrix. If an algebraic formula has to include the individual elements of the input matrix then it will not be compact. A method adopted here is to use not individual images but classes of inputs which can be represented in parametric fashion (see the notion of 'equivalence classes' below). In addition, input data has to fulfil an important requirement stated above, i.e. its parameters should occur explicitly in the model and be manipulated by it. Since the form of input data is closely related to the model expression and models can be enormously different from one another, solutions for this and the above problem are likely to remain non-generic.

3.2. Condition of constancy

Some of the above problems can be potentially overcome by introducing and exploiting the concept of the *condition of constancy*. In Section 1, we drew a parallel between the

parametrization problem in hand and the problem of recovery of an internal model for a given input–output [Eq. (1)]. We showed that when both the (computational) model and the parameters are undetermined, the solutions found can be ambiguous [Eqs. (3) and (4)]. This system analogy can also be applied to describe a psychophysical experiment, where $y(t)$ and $u(t)$ indicate, respectively, the input (a stimulus) and the output (the result) and $g(\mathbf{k})$ represents a part of visual system under scrutiny:

$$y(t) = g(\mathbf{k}) \otimes u(t).$$

A general approach of our method is to find the condition of constancy, i.e. to find a set of inputs $u(t)$ such that the output of the model remains fixed:

$$\forall t \in T \; y(t) = g(\mathbf{k}) \otimes u(t) = \text{const.} \tag{5}$$

The fulfilment of this condition leads to two system transformations which (subject to certain assumptions) can be fruitfully exploited. First, the condition of constancy in application to the model provides a means for factorization or elimination of parameters (system variables):

if $\forall t \in T \; y(t) = \text{const}$,

then (assuming associativity of $\otimes$),

$$\forall t_i, \; t_j \in T \; \exists \mathbf{k} \in K : \; 0 = y(t_i) - y(t_j) = g(\mathbf{k}) \otimes u(t_i) - g(\mathbf{k}) \otimes u(t_j) = g(\mathbf{k}) \otimes (u(t_i) - u(t_j)). \tag{6}$$

This is true when

1. $t_i = t_j$;
2. $u(t_i) = u(t_j)$;
3. the set of parameters K can be partitioned such that for its subsets K_1 and K_2:

$$K = K_1 \cup K_2 : \; g(\mathbf{k}_1) \otimes (u(t_i) - u(t_j)) = g(\mathbf{k}_2) \otimes (u(t_j) - u(t_i)), \; \mathbf{k}_1 \in K_1, \; \mathbf{k}_2 \in K_2.$$

Conditions 1 and 2 are trivial; condition 3 means that the parameters in K can be factorized (leading to a smaller parameter space) or eliminated.

The condition of constancy enables us also to partition inputs u into equivalence classes [34] such that two inputs are in the same class if and only if their outputs are equivalent, i.e. if and only if they are in the relationship λ, defined here as the condition of constancy:

$$(u(t_1), \; u(t_2)) \in \lambda \Leftrightarrow y(t_1) = y(t_2). \tag{7}$$

If we denote the fact that an experimental input $u(t_i)$ depends on the parameter vector $\mathbf{w}_i$ by:

$$u(t_i) = u(\mathbf{w}_i), \; \mathbf{w}_i \in W \subset R^k,$$

then we can observe that the condition of constancy partitions the set of parameters W into equivalence classes W/λ such that if two inputs $u(\mathbf{w}_i)$ and $u(\mathbf{w}_j)$, $i \neq j$, belong to the same equivalence class their outputs are indistinguishable. This is (trivially) the case when $\mathbf{w}_i = \mathbf{w}_j$. However, if V is a subspace of W and two inputs $u(\mathbf{w}_i)$, $u(\mathbf{w}_j)$ belong to the same equivalence class W/λ if they differ *only* by elements in V, then the set of inputs belonging to the same equivalence class can be generated using just the elements of subspace V and discarding all the others. Thus, the condition of constancy serves as a mechanism by which we can discard details of no interest and characterize suitable inputs in a concise manner (i.e. using only those parameters which belong to V).

The main building blocks of the method can be restated now as follows:

- seek psychophysical experiments which divide inputs into equivalence classes; determine a sub-space of the input parameter space which generates inputs belonging to the same equivalence class;
- use the condition of equivalence in application to the model to factor out or eliminate some of the model parameters;
- find values for the remaining model parameters by exploiting relationships between these parameters and the inputs and outputs of the psychophysical experiments identified above;
- evaluate the parametrized model by comparing its outputs with the equivalent outputs of the psychophysical experiments.

4. Parametrization of Neumann's model

4.1. Neumann's model

4.1.1. Background: Grossberg and Mingolla's model

The models of Grossberg and colleagues account for a very wide range of psychophysical phenomena with dynamic competitive/cooperative feedback networks of processing units, each of which is a mathematical model of some component of the brain. The model developed by Grossberg and Mingolla [4] suggests how contrasts and luminances in a scene might combine into visual percepts. In particular, they note that since human photoreceptors are partially obscured by retinal veins, the visual system must somehow be able to complete the gaps.

Fig. 3 (from Grossberg and Mingolla [3]) shows the macrocircuit of the monocular version of their model of human vision. The monocular pre-processing stage (MP) splits the image from the photoreceptors into contrast information and luminance information. The boundary contour system (BCS) generates continuous, sharp perceptual boundaries, parts of which are real (i.e. directly correspond to discontinuities in its input from the MP) and parts illusory (i.e. are completions of gaps in real boundaries). These perceptual boundaries are sent to the feature contour system (FCS) which allows colour and luminance information from the MP to diffuse through perceptual space until stopped by them. Note that it is the output from the FCS that is actually perceived, so the boundaries generated by the BCS are 'visible' only via the effect they have on the filling in

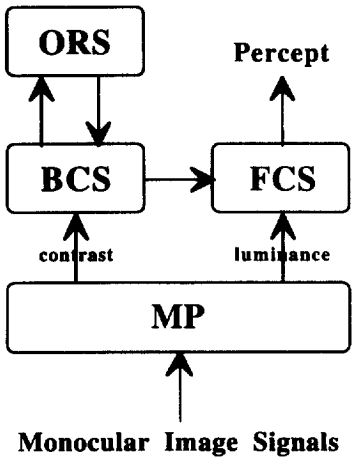

Fig. 3. Macrocircuit from Grossberg and Mingolla [3].

process of the FCS. Note also that the FCS cannot distinguish between real and illusory boundaries sent to it from the BCS: correspondingly, we are not aware of the completed gaps in our visual field. The object recognition system (ORS) recognizes objects from their perceptual boundaries alone and can also pass hypotheses to the BCS to help it complete the boundaries of recognized objects.

4.1.2. Motivation and architecture

Neumann [35,16] replaced the monocular pre-processing stage (MP) of Grossberg and Mingolla's model (MP in Fig. 3) with his own pre-processing stage (PP), as shown in Fig. 4. Recent neurophysiological research has shown that the retina and the striate cortex (V1 or area 17) are linked by two physically separate, parallel channels, called the ON-channel and the OFF-channel [36]. These channels comprise the axons of retinal ganglion cells and there is evidence (see Marr and Hildreth [5]) that these cells give some response to pure luminance information, as well as to ON- and OFF-contrast, respectively. Neumann's model, therefore, suggests a scheme whereby ON-contrast, OFF-contrast and luminance information are encoded into just these two channels by processing in the retina. The three streams of information are then decoded from the two channels by the striate cortex. The ON- and OFF-contrast information is then combined at each of several different orientations to provide the BCS with the approximate position and orientation of local contrast changes on the photoreceptors; the luminance information is contrast-enhanced and starts a diffusion process in the FCS.

The remainder of this section will focus on the parts of Neumann's model that lead to the position and orientation of contrast changes being fed into the BCS. The luminance information stream to the FCS will not be considered further, although it would be most important for any discussion of brightness phenomena. This cut-down model will be called 'Neumann's model' or simply 'the model' hereafter. Its input is a single, monochrome image, which is considered to be foveated.

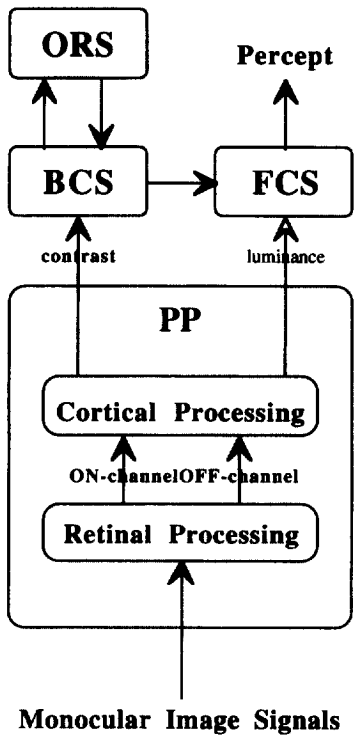

Fig. 4. Neumann's pre-processing stage in the context of Grossberg and Mingolla's model (Fig. 3).

4.1.3. Retinal processing

This section and the next will present a formal description of Neumann's [2] model,[4] giving the minimum detail needed to implement it computationally or analyse it mathematically.

The input to the model, $I(i, j)$, is first smoothed by two isotropic, normalized, low-pass filters: the smaller called the centre and the larger the surround. For example:

$$J^c(I) = I(i, j) \otimes \lambda^c(i, j) \text{ and } J^s(I) = I(i, j) \otimes \lambda^s(i, j), \quad (8)$$

where $\lambda^c(i, j) = (1/2\pi\sigma_c^2)e^{-(i^2+j^2)/2\sigma_c^2}$ and $\lambda^s(i, j) = (1/2\pi\sigma_s^2)e^{-(i^2+j^2)/2\sigma_s^2}$ (the superscript notation in the function names does not mean raised-to-the-power-of).

The outputs from both filters feed into each of two sets of ganglion cells whose axons form the ON- and OFF-channels, respectively. Their outputs, ${}^{\text{ON}}x(I)$ and ${}^{\text{OFF}}x(I)$, are each modelled by a shunting equation (Grossberg [37]). This first-order differential equation is assumed to be at its steady state and its outputs are set to zero wherever they become negative, so therefore:

$${}^{\text{ON}}x(I) = \left\lceil \frac{BJ^c(I) - CJ^s(I)}{A + J^c(I) + J^s(I)} \right\rceil \text{ and } {}^{\text{OFF}}x(I) = \left\lceil \frac{BJ^s(I) - CJ^c(I)}{A + J^c(I) + J^s(I)} \right\rceil, \quad (9)$$

[4] Our original work was based on the model described in the 1994 Technical Report. Its updated version was subsequently published in Neural Networks, 1996 [16]. Any changes to this more recent version of the model do not affect the main line of argument in this paper. The notation used in 1996 paper differs from the 1994; we follow here 1994 notation.

respectively (the half-brackets mean half-wave rectification).

4.1.4. Cortical processing

When the ON- and OFF-channel signals, ${}^{ON}x(I)$ and ${}^{OFF}x(I)$, arrive at the striate cortex, the ON- and OFF-contrasts, ${}^{ON}y(I)$ and ${}^{OFF}y(I)$, are decoded thus:

$$ {}^{ON}y(I) = \lceil {}^{ON}x(I) - {}^{OFF}x(I) \rceil \text{ and } {}^{OFF}y(I) = \lceil {}^{OFF}x(I) - {}^{ON}x(I) \rceil \tag{10}$$

(luminance is decoded by adding ${}^{ON}x(I)$ and ${}^{OFF}x(I)$ and is subsequently contrast-enhanced). The ON- and OFF-contrasts are, individually, separated into several different orientations by convolving each with the same set of elongated, normalized, Gaussian kernels:

$$ {}^{ON}y^{s}_{\varepsilon}(I) = {}^{ON}y(I) \otimes \lambda_{\varepsilon}(i, j) \text{ and}$$

$$ {}^{OFF}y^{s}_{\varepsilon}(I) = {}^{OFF}y(I) \otimes \lambda_{\varepsilon}(i, j), \tag{11}$$

where the $\lambda_{\varepsilon}(i,j)$ are described as "based on" $\lambda^{s}(i, j)$ but each elongated in the direction ε [16]. For example, $\lambda_{\varepsilon}(i, j)$ can be defined for each of the model's $2n$ orientations $\varepsilon = 0$, $\pi/2n,\ldots,(n-1)\pi/2n$ as the elongated, normalized Gaussian with size σ_e in the direction ε and size σ_s in the direction perpendicular to ε, i.e.:

$$ \lambda_{\varepsilon}(i, j) = \frac{1}{2\pi\sigma_e\sigma_s} e^{-(((i\cos\varepsilon - j\sin\varepsilon)^2/2\sigma_e^2) + ((i\sin\varepsilon - j\cos\varepsilon)^2/2\sigma_s^2))}. \tag{12}$$

The superscript 's' in the functions in Eq. (11) denotes 'simple': this stage models the action of simple cells in the hypercolumns of the striate cortex.

Finally, the output $O_{\varepsilon}(I)$ from the model at each orientation ε, is generated by summing the corresponding pair of functions from the sets defined in Eq. (11) and then convolving with the corresponding Gaussian kernel again:

$$ O_{\varepsilon}(I) = ({}^{ON}y^{s}_{\varepsilon}(I) + {}^{OFF}y^{s}_{\varepsilon}(I)) \otimes \lambda_{\varepsilon}(i, j). \tag{13}$$

These outputs model the outputs of cortical complex cells.

4.1.5. The parameters

There are five free parameters explicitly named in Neumann's description of the model: A, B, C, σ_c and σ_s. The first three come from the shunting equation used to model ganglion cells: A is the passive decay constant, B is the excitatory saturation constant and C is the inhibitory saturation constant and they are all non-negative (see Grossberg [37]). A controls the speed at which the shunting equation stabilizes, but the model assumes that this is fast enough, whatever A's value, to justify replacing the dynamic equation with its steady-state solution. Despite this, A still has effects on the model output, mainly on the subsequent compression of the range of luminances in the input. B and $-C$ are, respectively, the upper and lower bounds on the outputs from the shunting equation at its steady state. Billups [38] showed that in practice, the values of B and C only affect the output of the model by scaling it by $(B + C)$ and so these two parameters will not be considered any further in this paper.[5] The parameters σ_c and σ_s are introduced at the first stage of the model: they are the sizes of the centre and surround Gaussian filters, respectively. They correspond directly to the sizes of the centre and surround receptive fields of a retinal ganglion 'X' cell and therefore should be (much) greater than 0.01 degrees of visual angle (Hubel [39]). They are both strictly positive and σ_c must be strictly less than σ_s.

Finally, there are two other free parameters that were not explicitly named in Neumann's description of the model, but which will be denoted hereafter by $2n$ and σ_e. They are, respectively, the number of different orientations of elongated Gaussians used for filtering at the simple and complex cell stages of the model and the sizes of those elongated Gaussians along their longest axes. $2n$ must be strictly positive and should be even (so that every oriented Gaussian has another one perpendicular to it). The effect of this parameter will only be marked when the model is applied to images with edges that are not all vertical and horizontal. σ_e must be strictly greater than σ_s and has subtle effects on the behaviour of the model.

4.2. Using CSF data to rind a value for A

The three parameters for which parametrization is sought are A, σ_c and σ_s. The condition of constancy requires that a set of inputs $u(t)$ is found such that outputs $y(t)$ of the model g are constant. We have also noted that inputs should be specified parametrically so that they can be incorporated in the model's formula.

4.2.1. Condition of constancy

Algebraic analysis identified that a broad class of inputs of the form:

$$ I_i(x, y) = \alpha + \beta I_j(x, y),\ \alpha, \beta \in R, \tag{14}$$

can provide a condition of constancy for the Neumann's model. It can be shown that the model outputs $O(I_i)$ remain fixed, i.e.:

$$ O(I_i) = O(I_2) = \ldots = O(I_n),$$

if α and β are such that

$$ \beta = (2/A)\alpha + 1. \tag{15}$$

An important point to note is that the Eq. (15) involves the model parameter A. The formal proof of this is given in Appendix A.

This general form of input also points to a useful class of psychophysical experiments. The class of inputs characterized by the Eq. (14) is a set of images which differ by their mid-range luminance (an additive parameter α) and contrast

[5] Neumann [16] adopts a similar solution for B and C, although he supports it by different arguments.

(a multiplicative parameter β). With this interpretation of α and β within the condition of constancy, Eq. (15) states that in order for the output of the model to remain constant, image contrast c and its mid-range luminance m should be in the following relationship, involving the Neumann's model parameter A:

$$c = (2/A)m + 1. \tag{16}$$

This expression can be further transformed to:

$$c = (A/k)(1/m) + 2/k, \tag{17}$$

which states that in order for the output from Neumann's model to remain constant, the values of contrast and the reciprocals of the values of mid-range luminance of the two inputs must both lie on the same straight line, whose gradient divided by its intercept with the vertical axis must be $A/2$ (see Lemma 2 in Appendix A).

This enables us to make use of psychophysical experiments recording data about the contrast and mid-range luminance of otherwise identical stimuli.

4.2.2. CSF data

Having found a condition of constancy for the model, it is now necessary to find some psychophysical data to compare it with. This section will describe a psychophysical experiment to determine the conditions under which sinusoidal gratings are visible by human subjects and re-present data measured by De Valois et al. [40] in a suitable form.

The task of each subject in each trial of the experiment is to pick out the sinusoidal grating (the target stimulus) from among several, identical, uniform grey squares with the same mid-range luminance as the target (the distractor stimuli). The probability of the subject correctly picking out the grating is estimated at several different contrasts, spatial frequencies and mid-range luminances. (Contrast is defined here as $(L_{max} - L_{min})/(L_{max} + L_{min})$ and mid-range luminance as $(L_{max} + L_{min})/2$, where L_{max} and L_{min} are the highest and lowest luminances in a stimulus, respectively.) A threshold is chosen and the contrasts, spatial frequencies and mid-range luminances at which the probability of the subject correctly picking out the grating is exactly at this threshold are calculated. For example, the experimenters may decide that if the subject can correctly pick out the grating six times out of ten then it is just visible, in which case the contrasts, spatial frequencies and mid-range luminances at which the probability of the subject correctly picking out the grating is exactly 0.6 are calculated. The reciprocal of the minimum contrast at which a stimulus is visible is called its contrast sensitivity and Fig. 5 shows the contrast sensitivities of sinusoidal gratings as a function of their spatial frequencies at each of five different mid-range luminances. Such curves are called contrast sensitivity functions (CSFs) and those shown in Fig. 5 were measured by De Valois et al. [40].

The CSF data can be represented in a particular form: a fixed spatial frequency can be chosen and a graph plotted,

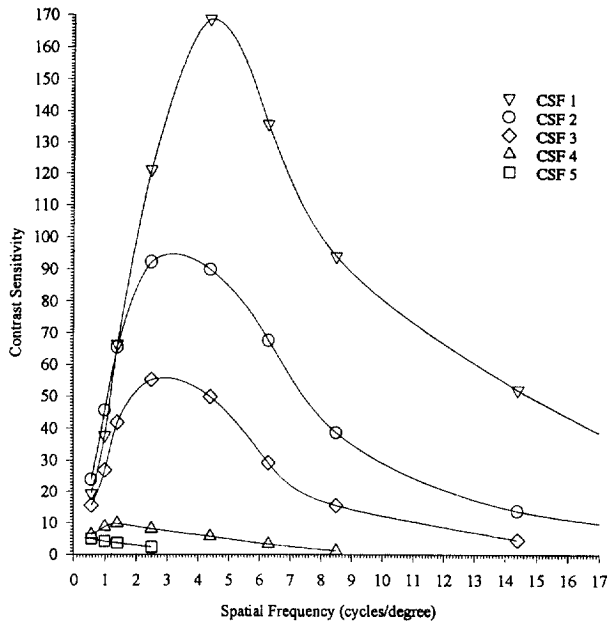

Fig. 5. CSFs 1–5 from Ref. [40], having mid-range luminances of 5, 0.5, 0.05, 0.005, and 0.0005 ft L respectively (17.13, 1.713, 0.1713, 0.01713, and 0.001713 candelas/m^2, respectively). Cubic spline curves have been fitted through the data points.

each of whose points represents the contrast and (reciprocal) mid-range luminance at which the probability of detection of the stimulus (at this particular spatial frequency) is at the threshold chosen by the experimenters. For example, Fig. 6 shows points of constant probability of detection in reciprocal mid-range luminance versus contrast space of stimuli of

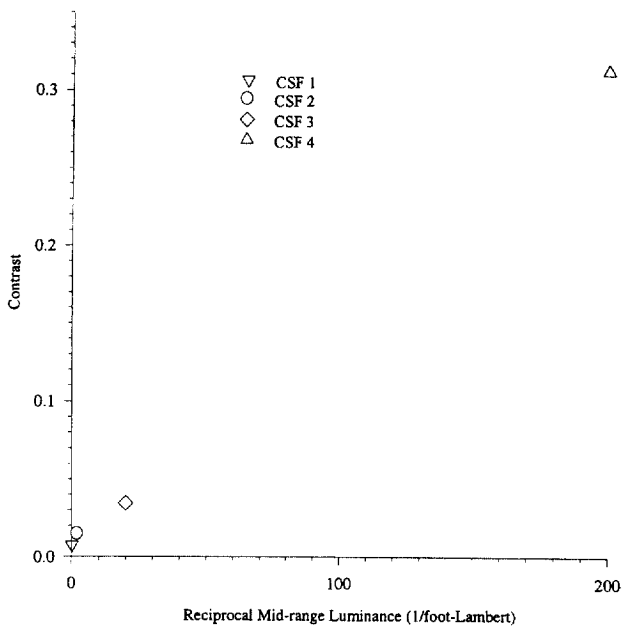

Fig. 6. Each point on this graph represents the contrast and reciprocal mid-range luminance at which the probability of detection of a grating of spatial frequency 6.3 cycles/degree is at the threshold chosen by the experimenters (1 ft L is 3.4263 candelas/m^2). CSF1–CSF4 refer to mid-range luminances of 5, 0.5, 0.05 and 0.005 ft L, respectively.

spatial frequency 6.3 cycles/degree. Note that these stimuli differ only in their contrast and mid-range luminance and thus fulfil the condition of constancy stated in the previous section.

4.2.3. Parametrization

The condition of constancy [Eq. (17)] identified above specifies a relationship between contrast and mid-range luminance:

$$c = (A/k)(1/m) + 2/k.$$

CSF data provides values for parameters c and m, thus, if the model is valid, a value of its parameter A can be recovered from the above relationship. Specifically, this relationship states that values of contrast plotted against reciprocal mid-range luminance should lie on a straight line whose gradient divided by its intercept with the vertical axis is $A/2$. If they don't then the model cannot explain the CSF data. Thus, plotting the CSF data at each spatial frequency independently (as in Fig. 6) and attempting to fit a straight line to them can both test the model and find values for the parameter A. (More accurate values for A could be found by using more CSFS, measured by different authors and at different mid-range luminances: the data points on Fig. 6 are a little sparse.)

4.2.4. Results

The procedure described above was performed at five of the eight different spatial frequencies for which enough data (i.e. contrast sensitivities at three or more different mid-range luminance levels) were available.[6] The criterion for the 'best line fit' was the minimization of the root-mean-squared relative error [38]. The De Valois data points, replotted in Fig. 7, had approximately linear arrangement, but the error for the best fitting line was quite large: 15% at spatial frequency 6.3 cycles/degree and 7–26% over the range of spatial frequencies 2.5–14.4 cycles/degree. These best fitting lines for each given frequency have been used to find approximate values for parameter A.

Fig. 8 shows the values of A derived from each of the different spatial frequencies. (At the higher spatial frequencies less data points are available: see Billups [38] for a precise description of how maximal use was made of the available data.)

The results shown in Fig. 8 are striking because the model states that A should be constant across all spatial frequencies. These data strongly suggest that A increases with spatial frequency and approximately linearly. However, since the model parameter A is analogous to a neurophysiological

[6] The lowest three spatial frequencies were ignored because the model certainly does not predict the fact that at these spatial frequencies detection can actually get *harder* with increasing mid-range luminance, as shown by the data. Whether or not this is an experimental error, perhaps due to the difficulty of foveating enough of a grating of low spatial frequency to see that it *is* a grating and whether or not these spatial frequencies can still be used in some way for parametrization remains to be investigated.

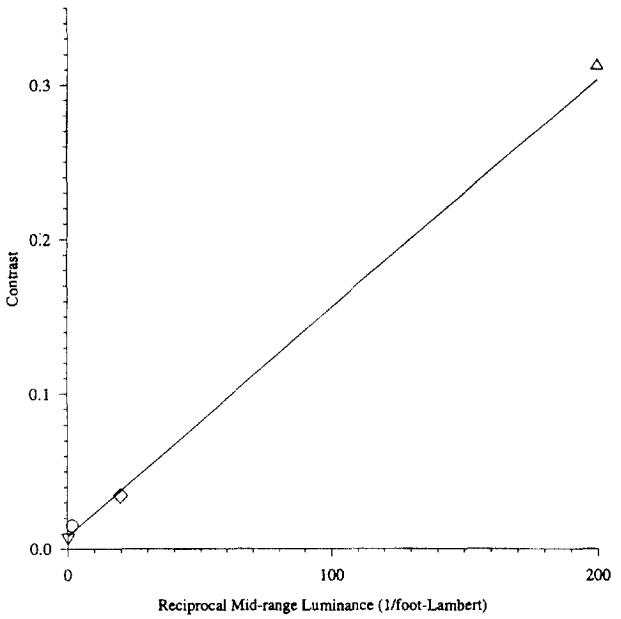

Fig. 7. The points of Eq. (6) with a straight line overlaid for comparison. The line is the minimum-root-mean-squared relative-error line through the points (error 15%).

constant in the retina (see Section 4.1.5), replacing it with a function of spatial frequency would compromise the biological plausibility of the model. An obvious alternative is to suggest that this particular part of the human visual system can be better modelled by multiple copies of the model, each centred on a different spatial frequency (as suggested by Neumann), but also having a different value of the

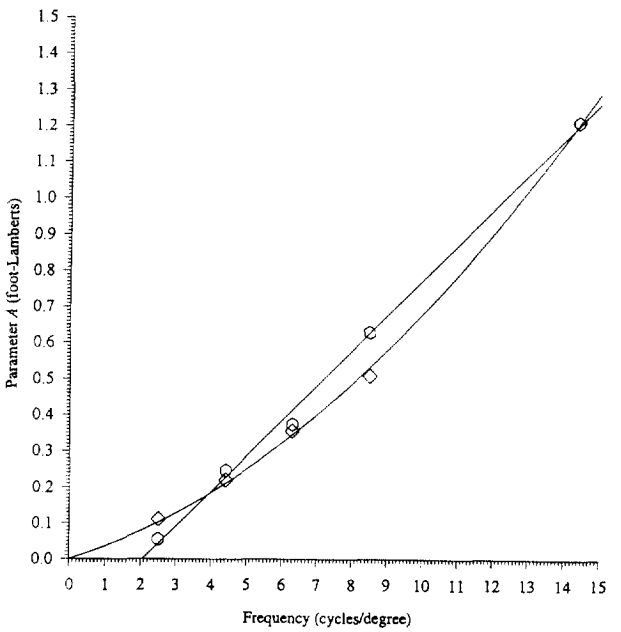

Fig. 8. The value of A found by fitting straight lines to the contrast versus reciprocal mid-range luminance data points at each of the different spatial frequencies. These values are shown with the minimum-root-mean-squared error line through them (hexagons). A curve overlaid over rhomboids is the best fitting curve with equation $A = 0.032F + 0.0036F^2$.

constant A. The method given here for setting the value of the parameter A has the advantage of using the data at each spatial frequency independently and so could parametrize each of these copies of the model.

In summary, it has been shown that the model does not match the CSF data at low spatial frequencies and that it matches the rest of the data only approximately. Furthermore, the choice of A such that the model optimally matches all five CSFs is not a constant but is the line $A = -0.2 + 0.1F$; if only the three CSFs with the highest mid-range luminances are considered then the optimal A is given by $A = 0.032F + 0.0036F^2$, where F is spatial frequency of the grating in cycles/degree. Both of these results are derived from the data at spatial frequencies between 2.5 and 14.4 cycles/degree. They cannot be extrapolated to lower spatial frequencies, but extrapolation to higher spatial frequencies may be possible.

Since the model would need changing substantially if it were to match the CSF data this analysis of the parameter A was not extended further, e.g. to find the ranges (as functions of spatial frequency) of values for A, as ideally should be done.

4.3. Using CSF data to find values for σ_c and σ_s

As for the parameter A, the first step is to find a condition of constancy, i.e. to identify a set of inputs and their appropriate parametric representations, such that the outputs from the model remain constant. The condition of constancy should involve σ_c and σ_s.

4.3.1. Condition of constancy for the model

Using a mixture of algebraic and numerical methods it was found that the condition of constancy can be specified for the class of inputs of the form

$$I(x, y) = m(1 + c\cos(fx)), \tag{18}$$

i.e. vertically oriented sinusoidal gratings. Many psychophysical experiments use such gratings as stimuli. For this class of inputs, the output $O_\varepsilon(x, y)$ from the model at each of its $2n$ orientations $\varepsilon = 0, \pi/2n, \ldots, (n-1)\pi/2n$ is an expression involving all the model parameters (as shown and proved in Appendix B). The following formula defines the peak heights of the model's vertically oriented output:

$$\max_{x,y}(O_{\pi/2}(x, y)) \approx (B + C)\left(\frac{mc}{A + 2m}\right)(e^{-\sigma_c^2 f^2/2} - e^{-\sigma_s^2 f^2/2}) \times \left(\frac{2}{\pi} + \left(1 - \frac{2}{\pi}\right)e^{-3.449(\sigma_s f)^{2.105}}\right). \tag{19}$$

This is an approximate formula which introduces an error that is typically less than 2% (although in exceptional circumstances the error can be as high as 6%). Derivation and proofs are shown in Appendix C and Appendix D.

The condition of constancy is that the peak heights (i.e. $\max(O_{\pi/2}(x, y))$) of the model's vertically oriented output remain fixed if the expression:

$$(B + C)\left(\frac{mc}{A + 2m}\right)(e^{-\sigma_c^2 f^2/2} - e^{-\sigma_s^2 f^2/2}) \times \left(\frac{2}{\pi} + \left(1 - \frac{2}{\pi}\right)e^{-3.449(\sigma_s f)^{2.105}}\right) \tag{20}$$

remains constant. This expression contains all the model parameters. However, as was argued elsewhere [38], $(B + C)$ is a scaling constant and A has been parametrized. The parameters m, c and f (mid-range luminance, contrast and frequency) provide a link between the model and the experimental data and σ_c and σ_s are parameters whose values are to be found.

The use of $\max(O_{\pi/2}(x, y))$ (peak heights) warrants further comment. According to Grossberg and Mingolla's description of their overall architecture, if a vertical grating is given as input then it is perceived when the peaks in the vertically oriented output from the BCS block horizontal diffusion in the FCS (see Fig. 3). Motivated by this, the output produced by the complete system is assumed to be a function of the vertically oriented output from Neumann's model, $O_{\pi/2}(x, y)$, alone. Furthermore, it is assumed to be a function of the heights of the regular peaks in $O_{\pi/2}(x, y)$.

4.3.2. CSF data

In this section, the CSF data of De Valois et al. [41] will be considered, presented in their more common form (refer back to Fig. 5). The most interesting feature of these curves, according to the experimenters, is the shift in their peaks towards the lower spatial frequencies as mid-range luminance is reduced. The lowest two CSFs are neglected here because their peaks occur at spatial frequencies that are too low. The spatial frequencies of the peaks of the remaining three CSFs have been estimated, from the cubic spline curves shown, to be 4.5, 3.2 and 2.9 cycles/degree. A crude upper bound for the absolute error introduced by this estimation process is 1.0 cycle/degree: the larger relative errors this implies for the more leftward peaks are justified by their flatter shapes.

Another important feature of the CSFs is their overall shape. One aspect of each CSF's shape can be quantified by estimating the spatial frequency at which contrast sensitivity has fallen by half after reaching its peak. These spatial frequencies have been estimated, again from the cubic spline curves of Fig. 5, to be 9.5, 7.6 and 6.4 cycles/degree for the three CSFs, respectively. Again, it is asserted that these values are accurate to within 1.0 cycle/degree. Finally, it should be noted that all six of these estimated spatial frequencies, each representing some feature of one of the CSFS, lie within the range 2.5–10.0 cycles/degree.

4.3.3. Parametrization

The condition of constancy for the model is that:

$$(B+C)\left(\frac{mc}{A+2m}\right)(e^{-\sigma_c^2 f^2/2} - e^{-\sigma_s^2 f^2/2}) \times \left(\frac{2}{\pi} + \left(1-\frac{2}{\pi}\right)e^{-3.449(\sigma_s f)^{2.105}}\right)$$

is fixed, or equivalently that

$$\frac{1}{c} \approx k(B+C)\left(\frac{m}{A+2m}\right)(e^{-\sigma_c^2 f^2/2} - e^{-\sigma_s^2 f^2/2}) \times \left(\frac{2}{\pi} + \left(1-\frac{2}{\pi}\right)e^{-3.449(\sigma_s f)^{2.105}}\right), \quad (21)$$

for some fixed k. As $1/c$ is, by definition, contrast sensitivity, this equation specifies a curve that can be directly compared with the CSF data. If Neumann's model explains the CSF data then each CSF will lie close to the corresponding curve for some values of the parameters σ_c and σ_s.

If when given two particular values for σ_c and σ_s the spatial frequencies of the peaks and of the half-peak heights of these curves lie within the ranges stated in section 4.3.2, then the model explains the data 'acceptably' with these parameter values. If no values for σ_c and σ_s generate an acceptable fit, then the model cannot explain the CSF data. Finally, the values of σ_c and σ_s that cause the peaks and half-peak heights of the curves to be 'closest' to those of the data will be called the 'optimal' values for those parameters. It should be noted that the spatial frequencies of the peaks and half-peak heights of the curves are independent of the unknown number k and the model parameters B and C and lie in the range of spatial frequencies in which the approximate Eq. (19) is most accurate.

4.3.4. Results

Firstly, observe from Eq. (21) that the curves corresponding to the CSFs (each of which just has a different value for m) will all peak at the same spatial frequency if A is constant. This is further confirmation that the model must be extended to multiple spatial scales as postulated earlier, although for the time being A is simply considered to be a function of spatial frequency. Since this section has considered only the first three CSFs the optimal A is $0.032F + 0.0036F^2$, where F is the spatial frequency of the input grating in cycles/degree.

To map out the values of σ_c and σ_s that cause the model to explain the data acceptably and optimally, the expression:

$$\left(\frac{m}{A+2m}\right)(e^{-\sigma_c^2 f^2/2} - e^{-\sigma_s^2 f^2/2}) \times \left(\frac{2}{\pi} + \left(1-\frac{2}{\pi}\right)e^{-3.449(\sigma_s f)^{2.105}}\right) \quad (22)$$

was repeatedly computed (using this optimal function for A and values for m of 5, 0.5 and 0.05 ft L). The results are shown in Fig. 9, which shows in particular that the optimal

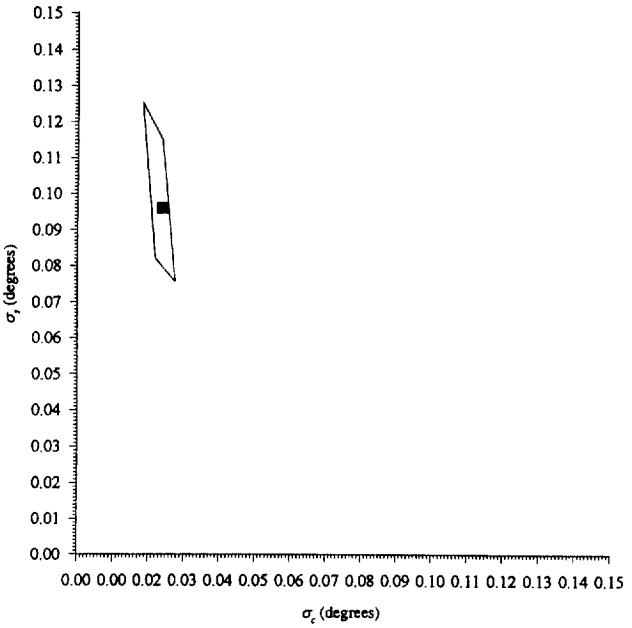

Fig. 9. The values of the parameters σ_c and σ_s that cause Neumann's model to explain the CSF data 'acceptably' (hollow region) and 'optimally' (solid square).

values of σ_c and σ_s are 0.024 and 0.096 degrees, respectively. As a check, it has been verified computationally that the errors introduced by the approximate Eq. (19) are well within their predicted limits given these values.

Although the use of the optimal function for A in calculating the optimal values for σ_c and σ_s is clearly reasonable, using it to calculate the acceptable values for them is not ideal. Other functions for A could be acceptable and could lead to other acceptable values for σ_c and σ_s. As a previous section did not find all the acceptable parametrizations for A (because it showed that A is not constant as the model assumes), this section cannot find all the acceptable values for σ_c and σ_s. The values illustrated in Fig. 9 should be regarded only as a guide. Should it be possible subsequently to find a range of acceptable functions for A, the method of this section could then find all the acceptable values for σ_c and σ_s.

4.4. Discussion

The analysis presented above made several assumptions related to CSF data which will be stated and discussed here. Although explicit references are made to the Neumann's model, the discussion is of a general nature.

4.4.1. Using CSF data to find a value for A

A fundamental assumption used in all the derivations so far was that the model could explain the CSF data. The approach used was to assume that it could, draw conclusions based on that assumption and then test those conclusions. If they were false then the model was called invalid (i.e. unable to explain the CSF data). This implies that a second

basic assumption was made: that the CSF data themselves were valid.

Further assumptions were also needed, some justification for which will be found here. As Neumann's model is a very general model of early vision and the CSF data measure human performance in a very specific experiment, the context of the model must be known in order to compare the two. Some information about the context of the model was explicit in Neumann's description of it, but some had to be assumed. For example, the rôle of the model within Grossberg and Mingolla's overall architecture led to the luminance information stream to the FCS being ignored. It was also assumed that Neumann's model accounted for the eye's optical apparatus. This could be loosely justified by remarking that the neural machinery of human vision has evolved to match the optical properties of the eye, as suggested by the similarity between the human CSF and modulation transfer function (De Valois and De Valois [41]). The assumption that Neumann's model accounted for the preprocessing of all the visual information subsequently used for detecting gratings was consistent with the rôle of the model since the luminance information stream to the FCS was ignored.

It was shown that the model is unable to explain the CSF data at low spatial frequencies, i.e. that it explains the rest of the CSF data only approximately and that the parameter A, described as a constant, must increase with the spatial frequency of the input grating. The optimal function of spatial frequency for A was found.

The analysis of the model implied that some preprocessing of its input, perhaps by a model of the optics of the eye, could cause the model to explain the CSF data more accurately (except at low spatial frequencies). It was also suggested that the model should be replicated at each of several different spatial scales: that way the parameter A of each replica could be a constant yet overall the As could increase with spatial frequency as required.

4.4.2. *Using CSF data to find values for* σ_c and σ_s

Two further assumptions were made about the context of the model, specifically about how its output is used to distinguish sinusoidal grating images at the threshold of visibility from uniform grey squares. Inspection of Eq. (19) shows that given a vertically oriented grating as input, the vertically oriented output from the model is always easier to detect than those of the other orientations, which are simply more blurred. However, to justify the assumption that only the peak heights of this output are used for subsequent detection, the analysis was repeated using several of its other features instead, such as the difference between its heights at its peaks and its troughs. It was found that as spatial frequency increased these features very rapidly became indistinguishable (in the presence of slight noise) from those of outputs given uniform square inputs. Using the peak heights of the vertically oriented output allowed gratings to be distinguished from uniform squares at higher spatial frequencies (although still not at the full range over which humans can perform this task).

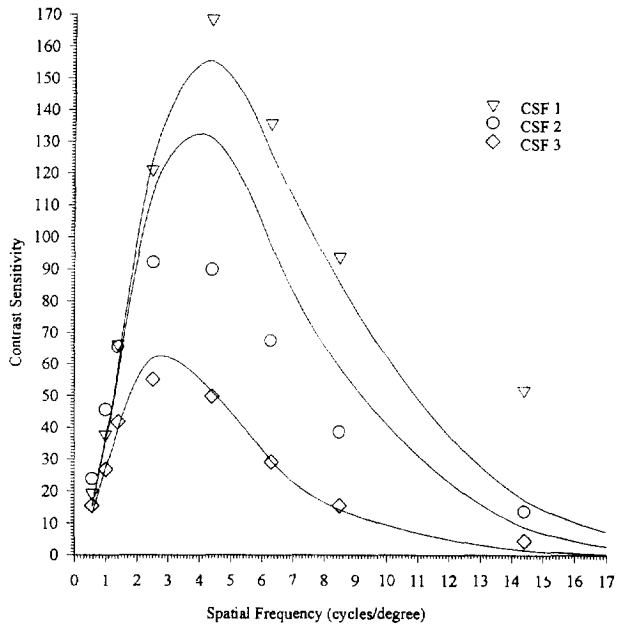

Fig. 10. The predictions of the parametrized model (lines) compared with the first three CSFs.

The results of parametrization of σ_c and σ_s confirmed that the parameter A must increase with the spatial frequency of the input grating and ranges in which the values of the parameters σ_c and σ_s must lie were found, as were their optimal values.

4.4.3. *A demonstration of the parametrized model*

One aim of parametrizing computational models is to implement them. While seeking the model parametrization it was assumed that the model could explain the data before parameter values necessary for this to be the case were found; but it was not shown that the model could explain the data even with these parameters. Therefore, the parametrized model has been implemented as a computer program and given grating stimuli as inputs. Fig. 10 shows how the behaviour of the parametrized model compares with the first three CSFS. It can be seen that the model's predictions of contrast sensitivity fall to zero much more quickly than the corresponding data do. Moreover, the predictions are not accurate at the higher spatial frequencies.

It is hypothesized here that a good way to solve this problem would be to specify less blurring in the later stages of the model [Eqs. (11) and (13)] to make the outputs easier to detect when high-frequency gratings are given as input.

5. Parametrization of Watt's model

5.1. *Watt's model*

Watt and his colleagues have developed a computational model of how the human visual system builds a symbolic

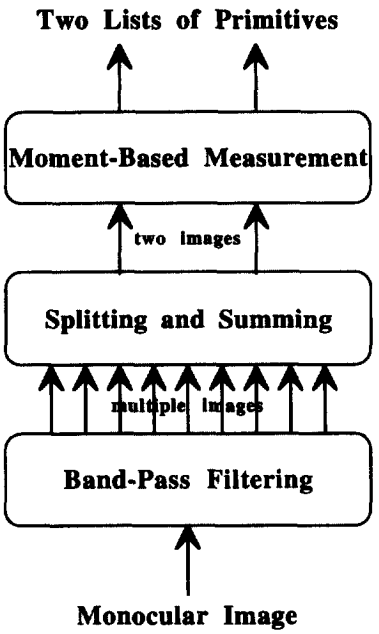

Fig. 11. Watt's model as a sequence of three high-level stages.

representation of luminance changes on the retina [17,18]. This representation must be sufficient for later visual processes to deduce the positions and properties of surfaces in the viewed scene, yet also as efficient (free from redundant information) as possible. The model takes as input a continuous function describing the luminance received at each point on one retina, i.e. a single, monochrome, monocular image. It has no prior knowledge of the viewed scene leading to this function and furthermore its first stage of processing deliberately introduces random noise, which affects the subsequent stages. Despite these difficulties, the model is robust and computationally efficient. Its output characterizes the magnitude, location and extent of luminance changes in its input and comprises two separate lists of discrete primitives, each primitive being a collection of three continuously variable attributes. There are rules that allow properties of the viewed scene to be deduced from this representation. The model may be thought of as a sequence of just three high-level stages, as illustrated in Fig. 11.

At the first stage of the model several copies of the input image are each convolved with a different band-pass filter kernel, i.e. the input is passed through several parallel channels, each of a different spatial frequency. Multiple channels give the model a wide overall bandwidth, and furthermore the outputs from this stage each have different desirable properties: some carry high spatial frequency information, while some, carrying only lower spatial frequency information, are less affected by the random noise (which is added, at this stage, to each output independently). The second stage first splits each of these outputs into a positive and a negative part. The positive part of an image is simply a copy of it with all its negative values replaced by zeros and the negative part is a copy with all its positive values replaced by zeros. The two outputs from this stage are the sum of the positive parts of all its inputs and the sum of the negative parts of all its inputs, respectively, and between them they retain all the important features of the several inputs (specifically, the locations and signs of their non-zero values) whilst having less noise and less redundancy. The outputs from the final stage are two lists of discrete primitives, each produced by taking moment-based measurements from its corresponding input: such measurements have been shown to be the most robust in the presence of noise [17]. It should be noted that this primitive-based representation is produced *after* the outputs from the first stage, i.e. of the frequency channels, have been combined. These outputs are not individually represented as collections of primitives and so are not individually accessible to later visual processes.

5.1.1. A definition of the model

There follows a mathematical definition of Watt's model, based on the descriptions in Refs [17,18]. The notation and the level of detail are those needed for the mathematical analysis later in this section.

At the first stage of the model, the input $I(x, y)$ is convolved with each of n band-pass spatial filters in turn:

$$F_i(x, y) = \left(1 - \frac{x^2 + y^2}{2\sigma_i^2}\right) e^{-(x^2+y^2)/2\sigma_i^2} \tag{23}$$

to give a response

$$R_i(x, y) = (F_i \otimes I)(x, y) \; i = 1, \ldots, n. \tag{24}$$

Importantly, the F_is are balanced: if the input is uniform, i.e. if $I(x, y) = m \; \forall x, y$, then the filters give no response, i.e. $R_i(x, y) = 0 \; \forall i, x, y$.

Although Watt always describes his model in terms of continuous functions, he states that in a computational implementation each function would be sampled at regularly spaced locations and replaced by a set of discrete values. Hereafter, all functions will be described discretely: to simplify the notation the same sampling interval, d, will be used throughout[7] and $(x, y) = (0,0)$ will be one of the sampling locations. For example, each of the responses $R_i(x, y)$ defined above will be described hereafter by an image R_i indexed by two integers j and k, i.e. as:

$$R_i(j, k) = (F_i \otimes I)(jd, kd) \; i = 1, \ldots, n;$$

$$j = \ldots, -1, 0, 1, \ldots; \; k = \ldots, -1, 0, 1, \ldots$$

At the end of this stage, intrinsic noise is modelled by adding to each response a random image $N_i(i, k)$ multiplied by a positive constant a. Each image N_i at each location (j, k) independently takes a value of the random variable N, which has expected value 0 and maximum amplitude 1 (so the

[7] Watt and Morgan [17] explain that the behaviour of the model is unchanged if different sampling intervals are used for each function. However, in their explanation they forget that when a function has noise added to every sample it becomes more unpredictable as its sampling rate is increased.

maximum amplitude of the intrinsic noise is a). After noise has been added, the responses of the filters are

$$R_i(j, k) + aN_i(j, k). \tag{25}$$

The second stage of the model first splits each of these noisy filter responses into a positive and a negative part (the half-brackets mean half-wave rectification):

$$R_i^+(j, k) = \lceil R_i(j, k) + aN_i(j, k) \rceil \text{ and}$$
$$R_i^-(j, k) = -\lceil -(R_i(j, k) + aN_i(j, k)) \rceil \tag{26}$$

and then sums the positive parts and the negative parts separately:

$$S^+(j, k) = \sum_{i=1}^{n} R_i^+(j,k) \text{ and } S^-(j, k) = \sum_{i=1}^{n} R_i^-(j, k). \tag{27}$$

If the model has uniform input then even though $R_i(i, k) = 0\ \forall i, j, k$ each of these sums still has a non-zero expected value: these are denoted s^+ and s^-, respectively. The final stage of the model takes moment-based measurements from the images $\lceil S^+(j, k) - s^+ \rceil$ and $-\lceil -(S^-(j, k) - s^- \rceil$ independently. Specifically, it represents every zero-bounded response distribution (i.e. region in which all the values are non-zero and that is bounded by values that are zero) in each image by a primitive having the following three continuously valued attributes: the mass, M, of the response distribution, its centroid, P, and its standard deviation, S.

At this point, it is necessary to state that Watt describes his model in one dimension only, even though he supports it with data from psychophysical experiments whose stimuli are two-dimensional. Hereto it has been straightforward to extend his description into two dimensions. Unfortunately, it is difficult to elegantly express algebraically what it means for a region of a two-dimensional set of discrete values to be 'zero-bounded' and so there are no simple formulae for the mass, centroid and standard deviation of the zero-bounded response distributions in an image. It is possible, up to a point, to define these attributes without defining 'zero-bounded', i.e. to define the attributes of a zero-bounded response distribution in terms of that zero-bounded region itself. For example, suppose the set Z is a zero-bounded region of the image $F(j, k)$. Then the mass, centroid and standard deviation of Z are:

$$M(F) = \lvert d^2 \sum_{(j,k)\in Z} F(j, k) \rvert,\ P(F) = (P_x(F),\ P_y(F))$$

$$= \left(\frac{\sum_{(j,k)\in Z} (jF(j, k))}{\sum_{(j,k)\in Z} F(j, k)}, \frac{\sum_{(j,k)\in Z} (kF(j, k))}{\sum_{(j,k)\in Z} F(j, k)} \right) \text{ and}$$

$$S(F) = (S_x(F),\ S_y(F))$$

$$= \left(\sqrt{\frac{\sum_{(j,k)\in Z} (j^2 F(j, k))}{\sum_{(j,k)\in Z} F(j, k)} - (P_x(F))^2}, \right.$$

$$\left. \sqrt{\frac{\sum_{(j,k)\in Z} (k^2 F(j, k))}{\sum_{(j,k)\in Z} F(j, k)} - (P_y(F))^2} \right). \tag{28}$$

Importantly, given a sampling interval, d, and some definition of 'zero-bounded', these attributes are functions of the image $F(j, k)$. This is true even if these attributes are made orientation-selective, as Watt and Morgan [17] suggest might be necessary when extending their model to two dimensions.

The output from the model, then, is two lists of discrete primitives, one for each of the images $\lceil S^+(j, k) - s^+ \rceil$ and $-\lceil -(S^-(j, k) - s^-) \rceil$. For every zero-bounded response distribution Z in each image there is a primitive with attributes mass, centroid and standard deviation.

5.1.2. The parameters

The definition of the model above contains several free parameters: the number, n and the sizes, $\sigma_1, \sigma_2, \ldots, \sigma_n$, of the spatial filters; the sampling interval, d, and the maximum amplitude, a, of intrinsic noise (all constants). In addition, the distribution of the random variable N is specified but only via its mean, 0 and maximum amplitude, 1. Watt and Morgan [17] specify that the spatial filter sizes range form 0.35 to 2.83 min of arc, but do not give the sizes in between or give values for the n, d and a.

5.1.3. Condition of constancy

Parametrization of Watt's model follows the same set of steps as parametrization of Neumann's model. Algebraic forms of both the model and the input are found to define the condition of constancy. The form of the input is the same here as for the derivation of parameter A in Neumann's model, i.e. inputs are taken from a general class of images which differ only in their contrast and mid-range luminance. However, there are two significant differences. Firstly, note that the condition of constancy is a condition on the input to a model that guarantees that its outputs remains fixed, yet the presence of random noise in Watt's model means that no condition on its input could ever guarantee that. The term 'stochastically equal' will be applied to random entities whose statistical properties are identical. The second new feature is that the condition of constancy initially does not involve the model's parameters. Hence in this form it can only test whether the model explains data.

The condition of constancy states that the model outputs remain stochastically equal if contrast c and mid-range

luminance m are such that:

$$c = k\frac{1}{m}, \tag{29}$$

i.e. values of c plotted against reciprocals of the values m must all lie on a straight line passing through the origin; detailed proof can be found in Billups [38]. This condition was tested using the CSF data and applying the same procedure as in the case of Neumann's model (see Section 4).

5.2. Results

The linear fit for CSF contrast and mid-range luminance data was carried out at five different spatial frequencies. The resulting root-mean-squared relative errors were very large, ranging from 59% to 74%. The error for the spatial frequency 6.3 cycles/degree was 61% (in comparison, the error associated with recovery of parameter A was 15%). This large error suggests that the Watt's model cannot explain the CSF data.

5.3. Developing and re-testing Watt's model

Watt and Morgan [17], citing Tolhurst et al. [42], propose that the maximum amplitude of intrinsic noise in their model might be a function of the mid-range luminance of the input, rather than being a constant. It seemed worthwhile to investigate whether such a development of the model can enable it to explain the CSF data. The inputs, as before, are required to differ only in their contrast and mid-range luminance. However, an additional condition is that a *particular* form of noise function is used, which assumes that noise increases linearly with increasing mid-range luminance of input:

$$a = p + qm, \text{ where } p,\ q \in R \text{ and } p,\ q > 0. \tag{30}$$

Thus, the maximum amplitude of intrinsic noise, a, is no longer assumed constant, but is a function of mid-range luminance, m. It can be proved [38] that the output of the model remains stochastically equal if, for the given class of inputs and the noise function $a = p + qm$, the following relationship is fulfilled:

$$c = kp\frac{1}{m} + kq. \tag{31}$$

Namely, the values of contrast and reciprocals of the values of mid-range luminance of the inputs must lie on the same straight line whose gradient divided by its intercept with the vertical axis equals p/q.

These predictions were tested against the CSF data, resulting in a much improved linear fit; the overall range of errors was 7–26%, with 15% error for spatial frequency 6.3 cycles/degree. Thus, a modified Watt's model, with a particular choice of noise function, explains the CSF data approximately. However, this version of the model seems to suffer from a similar problem as did Neumann's model, i.e. its parameter a appears to be a function of spatial frequency.[8]

5.4. Using one CSF to find a value for n

Although Watt's model cannot yet explain all the CSF data, it can explain individual CSFs. The remainder of this section will show how the technique can use a single CSF to find a value for the parameter n (i.e. the number of spatial frequency channels) in the original model. Less positively though, it will highlight a practical difficulty for the technique and its conclusions will be only tentative.

5.4.1. A hypothesized condition of constancy

The free parameters of Watt's model are n (the number of spatial frequency channels), $\sigma_2, \sigma_3, \ldots, \sigma_{n-1}$ (the sizes of the spatial filters in between σ_1 and σ_n which are fixed at 0.35 and 2.83 min of arc respectively), d (the sampling interval), a (the maximum amplitude of intrinsic noise) and the distribution of the random variable N (the intrinsic noise). The inputs are a class of sinusoidal gratings with the same mid-range luminance m but different contrasts c and n different spatial frequencies σ_i. The (hypothesized[9]) condition of constancy is that if the model is given the inputs as specified above, its outputs (defined as the values of the masses of its primitives divided by a) are stochastically equal if the contrast c and spatial frequency $f/2\pi$ of the corresponding input is such that:

$$K = \frac{cf}{a}\sum_{i=1}^{n}\sigma_i^4 e^{-\sigma_i^2 f^2/2} \tag{32}$$

is fixed. This is so whatever the value of d and the distribution of the random variable N.

In support of this hypothesis, Fig. 12 shows the mean of the normalized masses in the model's output plotted against values of expression 32, hereafter abbreviated to K, for a wide variety of different inputs and model parameters. If the hypothesis were exactly true, then for every different K the

[8] At each spatial frequency the value of p/q necessary for the model to explain the data may be calculated by dividing the gradient of the line best fitting the CSF data points by its intercept with the vertical axis. If the noise function is independent of frequency, the values of these quotients should be constant. However, this is not the case as p/q increases systematically with increasing frequency.

[9] This statement is a hypothesis rather than a theorem because the authors cannot yet prove it true. Eq. (32) was derived from exact algebraic formulae for band-pass filtered sinusoidal gratings by approximating the effect of each subsequent stage of the model. A mathematical analysis of the errors introduced by these approximations is extremely complex (because the random variables in the model mean that an algebraic description of the model must be in tenns of probability density functions rather than numerical variables). This highlights a practical difficulty for the technique: because it relies on mathematical analysis of models it is limited by the mathematical ability of whoever applies it. It is possible to imagine models so complex (particularly those whose output is partly random) that applying the technique would require a lot of very difficult work, even using powerful algebraic and numerical techniques and tools.

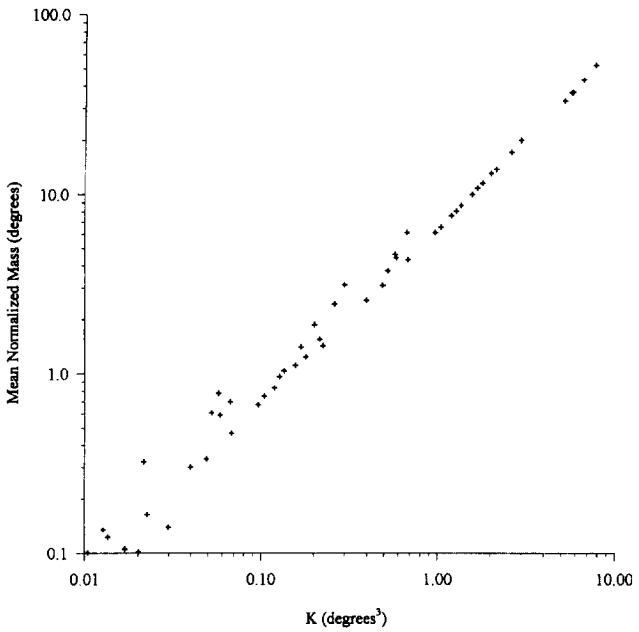

Fig. 12. In support of the hypothesis, this figure shows the mean of the normalized masses in the model's output plotted against values of K, for a wide variety of different inputs and model parameters. Specifically, the inputs had contrasts and spatial frequencies so as to be around the threshold of detection by humans (according to the CSF data), n varied between 2 and 50, the σ_is were assumed to be in geometric progression and a varied between 5×10^{-7} and 5×10^{-5} ft L. The model's output was computed for d between 5×10^{-4} and 5×10^{-2} degrees and for two different distributions of the random variable N.

mean normalized mass would be fixed whatever c, f, n, σ_2, $\sigma_3,\ldots,\sigma_{n-1}$, d, a and the distribution of N: the figure would show all the mean normalized masses lying on a curve that was a single-valued function of K.

For such a figure to prove the hypothesis true, points would have to be plotted for every possible combination of values of c, f, n, σ_2, $\sigma_3,\ldots,\sigma_{n-1}$, d, a and distribution of the random variable N. Furthermore, similar figures would be needed too for each of all the possible statistical properties of the masses in the model's output, other than just its mean. Clearly, the hypothesis cannot be proved this way. The rôle of Fig. 12 is to support the claim that the hypothesis is approximately valid for a wide variety of different inputs and model parameters, although the quality of the approximation and its dependence on those inputs and parameters is not yet known.

5.4.2. CSF data

To find the 'optimal' and 'acceptable' values for n two measurements characterizing CSF curves are used. These measurements, which had been used earlier in the Neumann's model, are the spatial frequency of the peak of each CSF and the spatial frequency at which contrast sensitivity had fallen by half after reaching its peak. In particular, the spatial frequencies of the peak and half-peak height of the CSF with mid-range luminance 5.0 ft L were estimated to be 4.5 ± 1.0 and 9.5 ± 1.0 cycles/degree, respectively. These two measurements can now be compared with the condition of constancy to find values for n.

5.4.3. Parametrization

The condition of constancy for the model is the condition that K [Eq. (32)] is fixed, or equivalently that:

$$\frac{1}{c} \approx k \frac{f}{a} \sum_{i=1}^{n} \sigma_i^4 e^{-\sigma_i^2 f^2/2} \tag{33}$$

for some fixed k. As $1/c$ is, by definition, contrast sensitivity, this condition clearly defines a curve that can be directly compared with a CSF. If Watt's model explains the first CSF then those data must lie close to a curve of the form of Eq. (33) for some value of the parameter n. (Since the σ_is are assumed to be in geometric progression, a value for n determines those of σ_2, $\sigma_3,\ldots,\sigma_{n-1}$.) If, when given a particular value for n, the spatial frequencies of the peak and the half-peak height of a curve of the form of Eq. (33) lie within the ranges stated earlier, then the model explains the data acceptably with that parameter value. (The spatial frequencies of the peak and half-peak height of the curves are independent of the unknown number k and the model parameter a.)

5.5. Tentative results

For a wide range of values of n, the spatial frequencies of the peak and the half-peak height of a curve of the form of Eq. (33) were computed and compared with the ranges stated in Section 5.4.3. This showed that Watt's model explained the data of the first CSF acceptably only if n was at least 4 and that no value of n caused the model to explain the data optimally because the curve and the data

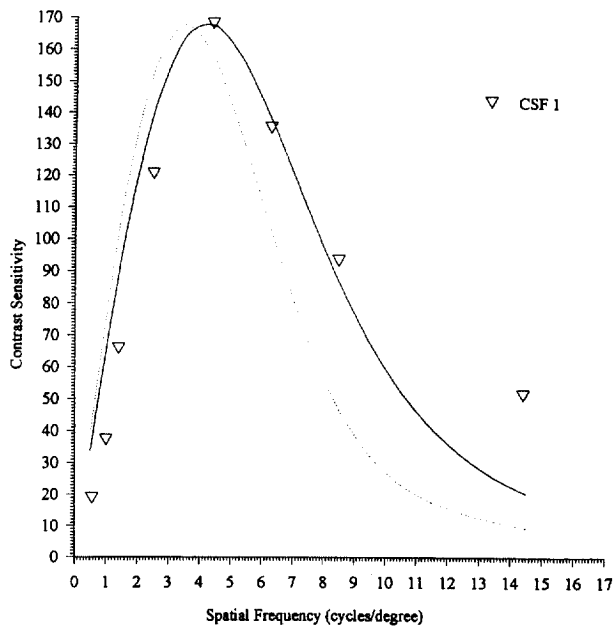

Fig. 13. The data of the first CSF compared with two curves of the form of Eq. (33), having n set to 4 (dotted line) and 40 (solid line), respectively.

got progressively closer if n was increased towards infinity. For example, Fig. 13 shows the data of the selected CSF compared with two curves of the form of Eq. (33), having n set to 4 and 40, respectively.

In summary, even though Watt's model cannot explain *all* the CSF data, it can explain *individual* CSFS. This section has shown how the parametrization technique based on the condition of constancy can use the first CSF to find a value for the parameter n. However, further investigation of the errors introduced in the derivation of the hypothesized condition of constancy is needed and so in the meantime the results of this section are only tentative.

6. General discussion

The authors' investigation of the problem of parametrization was first motivated by the difficulty of implementing an existing model. This difficulty was in part due to the common practice of publishing parameter values without discussion or justification, a practice that still prevails. The investigation involved the development of a new technique for parametrizing computational models of early vision.

The technique is broadly based on the concept of the recovery of an internal model for given input and output data. However, a novel key idea is the condition of constancy: a requirement to find input data such that the output of the model (or experiment) remains constant for the given data. This condition, in practice, makes it possible to manipulate both the model's variables and the input and experimental parameters so that the model itself can be evaluated against the given data. If the model can explain the data, it is further possible to find values for the model's parameters; if it cannot, trends in the erroneous responses may suggest how to modify the model so that it can explain the data. It should be noted also that the 'ground truth' psychophysical data is used it two ways: not only to evaluate the model (as it is usually used) but also to parametrize it.

The application of the parametrization technique was demonstrated for two different models of early vision. For Neumann's model the technique succeeded in deriving acceptable values for parameters σ_s and σ_c. The results of the attempted parametrization of A suggested that it may be a function of frequency, not a constant as given in the model. The technique applied to Watt's model showed that the model could not explain the CSF data. However, by modifying one of the model's noise function parameters, it was possible to derive the value for the number of spatial frequency channels and estimate the sizes of their respective spatial filters. In both cases the models were parametrized completely enough to allow them to be implemented. However, it is the authors' opinion that the development of a model, leading to its modification as a result of analysis of its initial responses, is more significant than the actual parameter values found: these values result from an illustrative demonstration of the technique using a relatively small sample of psychophysical data.

The principal limitation of the technique is that it cannot be stated in advance which models it can be successfully applied to and which it cannot. In the two demonstrations of the technique it was possible to find the conditions of constancy and the corresponding parametric form of image data. However, there are no guarantees that either exists. In general, choosing a class of inputs is largely a matter of mathematical convenience. For example, most models of early vision smooth their inputs, so choosing a class of inputs that can be still expressed algebraically after smoothing is a good idea (e.g. sinusoids, impulses, Gaussians, blurred step edges, but not sharp steps or triangular pulses). Many models assume linear early stages, so choosing a class of inputs that differ only in their contrast and mid-range luminance may also be useful. Manipulating functional descriptions of a model given an input from a particular class will often still require some mathematical simplifications and approximations.

Future work will concentrate on expressing the technique more formally, with the aim of stating when it can and cannot be applied. Some first steps towards this goal have been outlined by Billups [38].

Acknowledgements

This work was partially supported by the British–German Academic Research Collaboration Programme (project no. 285).

Appendix A Proof of Theorem 1

Lemma 1. *Let $O(I)$ denote the output from the model when given the input image $I(i, j)$. Suppose the model is successively given two inputs, $I_1(i, j)$ and $I_2(i, j)$,where $\exists \alpha,\beta \in \Re$ such that $I_2(i, j) = \alpha + \beta I_1(i, j)$ $\forall i, j$. Then $O(I_1) = O(I_2)$ $\forall i, j$ if $\beta = (2/A)\alpha + 1$.*

Proof. Consider the following function of the input to the model:

$$z(I) = \frac{B + C}{A + I(i, j) \otimes \lambda^c(i, j) + I(i, j) \otimes \lambda^s(i, j)} \times (I(i, j) \otimes \lambda^c(i, j) - I(i, j) \otimes \lambda^s(i, j)). \quad \text{(A.1)}$$

The lemma follows from the following two statements, which will be proved in turn. If the model is successively given two inputs, $I_1(i, j)$ and $I_2(i, j) = \alpha + \beta I_1(i, j)$ where $\beta = (2/A)\alpha + 1$, then $z(I_1) = z(I_2)$ $\forall i, j$. If $z(I_1) = z(I_2)$ $\forall i, j$ then $O(I_1) = O(I_2)$ $\forall i, j$.

If the model is given input $I_2(i,j)$, then from the definition in Eq. (A.1):

$$z(I_2) = \frac{B+C}{A + I_2(i,j) \otimes \lambda^c(i,j) + I_2(i,j) \otimes \lambda^s(i,j)} \times (I_2(i,j) \otimes \lambda^c(i,j) - I_2(i,j) \otimes \lambda^s(i,j)). \quad \text{(A.2)}$$

If $I_2(i,j) = \alpha + \beta I_1(i,j)$ then since convolution is linear and the kernels $\lambda^c(i,j)$ and $\lambda^s(i,j)$ are normalized, $I_2(i,j) \otimes \lambda^c(i,j) = \alpha + \beta I_1(i,j) \otimes \lambda^c(i,j)$. Substituting this into Eq. (A.2):

$$z(I_2) = \frac{B+C}{A + 2\alpha + \beta(I_1(i,j) \otimes \lambda^c(i,j) + I_1(i,j) \otimes \lambda^s(i,j)) \times \beta(I_1(i,j) \otimes \lambda^c(i,j) - I_1(i,j) \otimes \lambda^s(i,j))}$$

$$= \frac{B+C}{\{(A+2\alpha)/\beta\} + I_1(i,j) \otimes \lambda^c(i,j) + I_1(i,j) \otimes \lambda^s(i,j) \times (I_1(i,j) \otimes \lambda^c(i,j) - I_1(i,j) \otimes \lambda^s(i,j)).}$$

If $\beta = (2/A)\alpha + 1$, $\{(A + 2\alpha)/\beta\} = A$ and so:

$$z(I_2) = \frac{B+C}{A + I_1(i,j) \otimes \lambda^c(i,j) + I_1(i,j) \otimes \lambda^s(i,j)) \times (I_1 \otimes \lambda^c(i,j) - I_1(i,j) \otimes \lambda^s(i,j)) = z(I_1) \forall i,j.}$$

To see how this implies that $O(I_1) = O(I_2) \forall i,j$, consider the following two functions defined by Neumann [2]:

$${}^{\text{ON}}y(I) = \frac{B+C}{A + I(i,j) \otimes \lambda^c(i,j) + I(i,j) \otimes \lambda^s(i,j) \times [I(i,j) \otimes \lambda^c(i,j) - I(i,j) \otimes \lambda^s(i,j))]} \text{ and}$$

$${}^{\text{OFF}}y(I) = \frac{B+C}{A + I(i,j) \otimes \lambda^c(i,j) + I(i,j) \otimes \lambda^s(i,j) \times [I(i,j) \otimes \lambda^s(i,j) - I(i,j) \otimes \lambda^c(i,j)].} \quad \text{(A.3)}$$

Since the model requires that A, B, C, $I(i,j)$, $\lambda^c(i,j)$ and $\lambda^s(i,j)$ are positive ($\forall i,j$), comparison between Eqs. (A.3) and (A.1) shows that:

$${}^{\text{ON}}y(I) = [z(I)] \text{ and } {}^{\text{OFF}}y(I) = [-z(I)] \; \forall i,j,$$

and so if $z(I_1) = z(I_2) \forall i,j$ then ${}^{\text{ON}}y(I_1) = {}^{\text{ON}}y(I_2)$ and ${}^{\text{OFF}}y(I_1) = {}^{\text{OFF}}y(I_2) \forall i,j$. It follows from Neumann's subsequent description of the model (see Section 4.1.4 or Neumann [2]), in which the output from the model depends on its input *only* via the two intermediate functions ${}^{\text{ON}}y(I)$ and ${}^{\text{OFF}}y(I)$, i.e. that if ${}^{\text{ON}}y(I_1) = {}^{\text{ON}}y(I_2)$ and ${}^{\text{OFF}}y(I_1) = {}^{\text{OFF}}y(I_2) \forall i,j$ then $O(I_1) = O(I_2) \forall i,j$.

Lemma 2. *Let $O(I)$ denote the output from the model when given the input image $I(x,y)$. Suppose the model is successively given two inputs, $I_1(i,j)$ and $I_2(i,j)$, where $\exists \alpha, \beta \in \Re$, $\beta > 0$, such that $I_2(i,j) = \alpha + \beta I_1(i,j) \forall i,j$. Furthermore, suppose that $I_1(i,j)$ has contrast c_1 and mid-range luminance m_1 and $I_2(i,j)$ has contrast c_2 and mid-range luminance m_2. Then $O(I_1) = O(I_2) \forall i,j$ if $\exists k \in \Re$ such that $c_1 = (A/k)(1/m_1) + (2/k)$ and $c_2 = (A/k)(1/m_2) + (2/k)$.*

Proof. By the definitions of mid-range luminance and contrast:

$$m_1 = \frac{\max_{i,j}(I_1(i,j)) + \min_{i,j}(I_1(i,j))}{2},$$

$$c_1 = \frac{\max_{i,j}(I_1(i,j)) - \min_{i,j}(I_1(i,j))}{\max_{i,j}(I_1(i,j)) + \min_{i,j}(I_1(i,j))},$$

$$m_2 = \frac{\max_{i,j}(I_2(i,j)) + \min_{i,j}(I_2(i,j))}{2} \text{ and}$$

$$c_2 = \frac{\max_{i,j}(I_2(i,j)) - \min_{i,j}(I_2(i,j))}{\max_{i,j}(I_2(i,j)) + \max_{i,j}(I_2(i,j))}.$$

Because $I_2(i,j) = \alpha + \beta I_1(i,j)$:

$$\max_{i,j}(I_2(i,j) = \begin{cases} \alpha + \beta \max_{i,j}(I_1(i,j) \text{ if } \beta \geq 0 \\ \alpha + \beta \min_{i,j}(I_1(i,j) \text{ if } \beta < 0 \end{cases} \text{ and}$$

$$\min_{i,j}(I_2(i,j) = \begin{cases} \alpha + \beta \min_{i,j}(I_1(i,j) \text{ if } \beta \geq 0 \text{ and} \\ \alpha + \beta \max_{i,j}(I_1(i,j) \text{ if } \beta < 0 \end{cases}$$

but since $\beta > 0$ it is simple to show that

$$m_2 = a + \beta m_1 \text{ and } c_2 = \frac{\beta m_1 c_1}{\alpha + \beta m_1}. \quad \text{(A.4)}$$

If $c_1 = (A/k)(1/m_1) + (2/k)$ and $c_2 = (A/k)(1/m_2) + (2/k)$, then:

$$\frac{m_1 c_1}{m_2 c_2} = \frac{A + 2m_1}{A + 2m_2},$$

which, substituting in Eq. (A.1), gives

$$\frac{m_1 c_1}{(\alpha + \beta m_1)\left(\frac{\beta m_1 c_1}{\alpha + \beta m_1}\right)} = \frac{A + 2m_1}{A + 2(\alpha + \beta m_1)},$$

i.e.

$$\beta = (2/A).\alpha + 1.$$

So by Lemma 1, $O_1(i,j) = O_2 \forall i,j$.

Theorem 1. *Suppose Neumann's model is successively given several inputs that differ only in their contrast and mid-range luminance. Suppose the contrast of each image is plotted against the reciprocal of its mid-range luminance on a single graph. Then the successive outputs from the model will be identical if these points lie on any one of a particular family of straight lines. This family comprises those lines whose gradient divided by their intercept with the vertical axis equals half the value of the model parameter A.*

The Theorem 1 notation (of Lemmas 1 and 2) is as follows. Let $O(I)$ denote the output from the model when given the input image $I(x,y)$. Suppose Neumann's model is

successively given n inputs, $I_1(i, j)$, $I_2(i, j)$,...,$I_n(i, j)$, where for each pair $I_p(i, j)$ and $I_q(i, j)$ $\exists \alpha_{pq}, \beta_{pq} \in \Re$, $\beta_{pq} > 0$, such that $I_p(i, j) = \alpha_{pq} + \beta_{pq} I_q(i, j) \forall i, j$. Then $O(I_1) = O(I_2) = \cdots = O(I_n) \forall i, j$ if $\exists k \in \Re$ such that $c_1 = (A/k)(1/m_1) + (2/k)$, $c_2 = (A/k)(1/m_2) + (2/k)$,...,$c_n = (A/k)(1/m_n) + (2/k)$.

Proof. Suppose that $\exists k \in \Re$ such that $c_1 = (A/k)(1/m_1) + (2/k)$, $c_2 = (A/k)(1/m_2) + (2/k)$,...,$c_n = (A/k)(1/m_n) + (2/k)$. Now arbitrarily choose a pair of inputs $I_p(i, j)$ and $I_q(i, j)$.

Because $\exists \alpha_{pq}, \beta_{pq} \in \Re$, $\beta_{pq} > 0$, such that $I_p(i, j) = \alpha_{pq} + \beta_{pq} I_q(i, j) \forall i, j$ and $\exists k \in \Re$ such that $c_p = (A/k)(1/m_p) + (2/k)$ and $c_q = (A/k)(1/m_q) + (2/k)$, Lemma 2 implies that $O(I_p) = O(I_q) \forall i, j$. So, by choosing the $n - 1$ pairs $I_1(i, j)$ and $I_2(i, j)$, $I_2(i, j)$ and $I_3(i, j)$,...,$I_{n-1}(i, j)$ and $I_n(i, j)$, it is simple to show that $O(I_1) = O(I_2) = \cdots = O(I_n) \forall i, j$ and so the theorem is proved.

Appendix B Proof of Theorem 2

Lemma 3:

$$\int_{\Re} e^{-(x+ib)^2}\, dx = \sqrt{\pi}\ \forall b \in \Re.$$

Abbreviated proof. The integral of the function e^{-z^2} around the rectangle having vertices $-a$, a, $a + ib$ and $-a + ib$ (where $z = x + iy$ and x, y, a and $b \in \Re$) must equal zero (by Cauchy's integral theorem). In the limit $a \to \infty$, this equality simplifies to:

$$\int_{\Re} e^{-(x+ib)^2}\, dx = \int_{\Re} e^{-x^2}\, dx,$$

whose right-hand side is well known to have the value $\sqrt{\pi}$. See Ref. [38] for the full proof of all the lemmas in this Appendix.

Lemma 4:

$$\int_{\Re} e^{-px^2} \cos(qx)\, dx = \frac{\sqrt{\pi}}{\sqrt{p}} e^{-q^2/4p}\ \forall p > 0.$$

Abbreviated proof. This integral is evaluated by expressing the cosine term as a complex exponential (by the Euler formula), substituting x for $\sqrt{p}x$ and then applying Lemma 3.

Lemma 5

$$\int_{\Re} \cos(qx)\, dx = 2\pi\delta(q).$$

Abbreviated proof. Strictly, this integral does not converge and is only meaningful to mathematicians in the context of distribution theory. To avoid a rather abstract discussion, we note that for all practical purposes this integral may be interpreted as the limit of a sequence of integrals that do converge. For example, we can define it thus:

$$\int_{\Re} \cos(qx)\, dx = \lim_{p \to 0} \left(\int_{\Re} e^{-px^2} \cos(qx)\, dx \right), \text{ where } p > 0.$$

These integrals are evaluated by applying Lemma 4, substituting σ^2 for $2p$ and then noting that a Gaussian in the limit $\sigma \to 0$ is a delta function.

Lemma 6:

$$\cos(fx) \otimes \frac{1}{\sqrt{2\pi\sigma^2}} e^{-x^2/2\sigma^2} = e^{-\sigma^2 f^2/2} \cos(fx).$$

Abbreviated proof. Fourier transforms of the two sides of this equality are shown to be identical.

$$F(f) = \int_{\Re} f(x) \cos(ax)\, dx$$

is chosen as the transform, so that

$$F\left(\cos(fx) \otimes \frac{1}{\sqrt{2\pi\sigma^2}} e^{-x^2/2\sigma^2} \right) = \pi(\delta(f + a) + \delta(f - a)) e^{-\sigma^2 f^2/2}$$

(using the product-of-cosines formula and Lemmas 4 and 5). Similar calculations also show that:

$$F(e^{-\sigma^2 f^2/2} \cos(fx)) = \pi(\delta(f + a) + \delta(f - a)) e^{-\sigma^2 f^2/2}.$$

Lemma 7. *Let $g(x, y)$ be the convolution of an image $f(x, y)$ with the normalized two-dimensional Gaussian with size σ_ε in the direction ε and size σ_s in the direction perpendicular to ε. If $f(x, y)$ varies only in the x direction (i.e. if $f(x, y)$ is independent of y) then:*

$$g(x, y) = f(x, y) \otimes \frac{1}{\sqrt{2\pi_\varepsilon \sigma^2}} e^{-x^2/2\sigma_\varepsilon^2},$$

where $\sigma_\varepsilon^2 = \sigma_\varepsilon^2 \cos^2\varepsilon + \sigma_s^2 \sin^2\varepsilon$.

Abbreviated proof. Since $f(x, y)$ is independent of y, it is simple to show that:

$$g(x, y) = f(x, y) \otimes \int_{\Re} \lambda_\varepsilon(u, v)\, dv,$$

where $\lambda_\varepsilon(x, y)$ is the Gaussian kernel. To prove the lemma, the integral is evaluated using an obvious but complicated substitution and the same well-known integral as in the proof of Lemma 3.

Lemma 8:

$$\frac{1}{\sqrt{2\pi\sigma_p^2}}e^{-x^2/2\sigma_p^2} \otimes \frac{1}{\sqrt{2\pi\sigma_q^2}}e^{-x^2/2\sigma_q^2} = \frac{1}{\sqrt{2\pi\sigma_r^2}}e^{-x^2/2\sigma_r^2},$$

where $\sigma_r^2 = \sigma_p^2 + \sigma_q^2$.

Abbreviated proof. This convolution is written as an integral, which is evaluated using an obvious but complicated substitution and the same well-known integral as in the proof of Lemma 3.

Theorem 2. *Suppose the input to Neumann's model is a sinusoidal grating with mid-range luminance m, contrast c and spatial frequency $f/2\pi$:*

$$I(x, y) = m(1 + c\cos(fx))$$

then the output from the model at each of its $2n$ orientations $\varepsilon = 0, \pi/2n, \ldots, (n-1)\pi/2n$ will be

$$O_\varepsilon(x, y) = \left| \frac{(B+C)(e^{-\sigma_c^2 f^2/2} - e^{-\sigma_s^2 f^2/2})\cos(fx)}{\frac{A+2m}{mc} + (e^{-\sigma_c^2 f^2/2} + e^{-\sigma_s^2 f^2/2})\cos(fx)} \right| \otimes \left(\frac{1}{\sqrt{4\pi(\sigma_c^2\cos^2\varepsilon + \sigma_s^2\sin^2\varepsilon)}} e^{-x^2/4(\sigma_c^2\cos^2\varepsilon + \sigma_s^2\sin^2\varepsilon)} \right),$$

where A, B, C, σ_c and σ_s, (all positive) are the free parameters of the model and $\sigma_c > \sigma_s$.

Proof. Consider the following two functions defined by Neumann [2]:

$$^{\mathrm{ON}}y(I) = \frac{B+C}{A + I(x, y) \otimes \lambda^c(x, y) + I(x, y) \otimes \lambda^s(x, y)} \times [I(x, y) \otimes \lambda^c(x, y) - I(x, y) \otimes \lambda^s(x, y))] \text{ and}$$

$$^{\mathrm{OFF}}y(I) = \frac{B+C}{A + I(x, y) \otimes \lambda^c(x, y) + I(x, y) \otimes \lambda^s(x, y)} \times [I(x, y) \otimes \lambda^s(x, y) - I(x, y) \otimes \lambda^c(x, y)], \quad \text{(B.1)}$$

where $\lambda^c(x, y) = (1/2\pi\sigma_c^2)e^{-(x^2+y^2)/2\sigma_c^2}$, $\lambda^s(x, y) = (1/2\pi\sigma_s^2)e^{-(x^2+y^2)/2\sigma_s^2}$ and A, B, C, σ_c and σ_s, are the free parameters of the model. Two sets of new functions are derived by convolving each of the functions of Eq. (B.1) with the same set of Gaussian kernels (see Ref. [2]):

$$^{\mathrm{ON}}y_\varepsilon^s(I) = {}^{\mathrm{ON}}y(I) \otimes \lambda_\varepsilon(x, y) \text{ and}$$

$$^{\mathrm{OFF}}y_\varepsilon^s(I) = {}^{\mathrm{OFF}}y(I) \otimes \lambda_\varepsilon(x, y), \quad \text{(B.2)}$$

where the $\lambda_\varepsilon(x, y)$ are described as "based on" $\lambda^s(x, y)$ but each elongated in the direction ε. We formalize Neumann's description by defining $\lambda_\varepsilon(x, y)$ for each of the model's $2n$ orientations $\varepsilon = 0, \pi/2n, \ldots, (n-1)\pi/2n$ as the normalized two-dimensional Gaussian with size σ_c in the direction ε and size σ_s, in the direction perpendicular to ε, i.e.:

$$\lambda_\varepsilon(x, y) = \frac{1}{2\pi\sigma_c\sigma_s} e^{-((x\cos\varepsilon - y\sin\varepsilon)^2/2\sigma_c^2 + (x\sin\varepsilon - y\cos\varepsilon)^2/2\sigma_s^2)}.$$

Neumann [2] next describes how the output from the model at each orientation ε, $O_\varepsilon(I)$, is generated by summing the corresponding pair of functions from the sets defined in Eq. (B.2) and then convolving with the corresponding Gaussian kernel again:

$$\begin{aligned} O_\varepsilon(I) &= ({}^{\mathrm{ON}}y_\varepsilon^s(I) + {}^{\mathrm{OFF}}y_\varepsilon^s(I)) \otimes \lambda_\varepsilon(x, y) \\ &= ({}^{\mathrm{ON}}y(I) \otimes \lambda_\varepsilon(x, y) \\ &\quad + {}^{\mathrm{OFF}}y(I) \otimes \lambda_\varepsilon(x, y)) \otimes \lambda_\varepsilon(x, y). \end{aligned}$$

Equivalently,

$$O_\varepsilon(I) = ({}^{\mathrm{ON}}y(I) + {}^{\mathrm{OFF}}y(I)) \otimes \lambda_\varepsilon(x, y) \otimes \lambda_\varepsilon(x, y). \quad \text{(B.3)}$$

To prove the theorem we evaluate the right-hand side of Eq. (B.3), starting with the term $({}^{\mathrm{ON}}y(I) + {}^{\mathrm{OFF}}y(I))$. Firstly, we note that from Eq. (B.1) that:

$$^{\mathrm{ON}}y(I) + {}^{\mathrm{OFF}}y(I) = \frac{B+C}{A + I(x, y) \otimes \lambda^c(x, y) + I(x, y) \otimes \lambda^s(x, y)} \times |I(x, y) \otimes \lambda^c(x, y) - I(x, y) \otimes \lambda^s(x, y)| \quad \text{(B.4)}$$

and since the model's parameters, input and kernels are all positive,

$$\begin{aligned} &{}^{\mathrm{ON}}y(I) + {}^{\mathrm{OFF}}y(I) \\ &= \left| \frac{(B+C)(I(x, y) \otimes \lambda^c(x, y) - I(x, y) \otimes \lambda^s(x, y))}{A + I(x, y) \otimes \lambda^c(x, y) + I(x, y) \otimes \lambda^s(x, y)} \right|. \end{aligned}$$

Secondly, we note that $I(x, y)$ varies only in the x direction and $\lambda^c(x, y)$ is the normalized two-dimensional Gaussian with size σ_c in all directions, so from Lemma 7:

$$\begin{aligned} I(x, y) \otimes \lambda^c(x, y) &= I(x, y) \otimes \frac{1}{\sqrt{2\pi\sigma_c}} e^{-x^2/2\sigma_c} \\ &= m(1 + c\cos(fx)) \otimes \frac{1}{\sqrt{2\pi\sigma_c}} e^{-x^2/2\sigma_c} \\ &= m\left(\int_{\Re} \frac{1}{\sqrt{2\pi\sigma_c}} e^{-x^2/2\sigma_c} \, dx \right. \\ &\quad \left. + \left(c\cos(fx) \otimes \frac{1}{\sqrt{2\pi\sigma_c}} e^{-x^2/2\sigma_c} \right) \right) \\ &= m\left(1 + c\left(\cos(fx) \otimes \frac{1}{\sqrt{2\pi\sigma_c}} e^{-x^2/2\sigma_c} \right) \right) \\ &= m(1 + ce^{-\sigma_c^2 f^2/2}\cos(fx)) \text{ (Lemma 6).} \end{aligned}$$

Similarly,

$$I(x, y) \otimes \lambda^s(x, y) = m(1 + ce^{-\sigma_s^2 f^2/2}\cos(fx)).$$

Putting these into Eq. (B.4), we have:

$$\begin{aligned} &{}^{\mathrm{ON}}y(I) + {}^{\mathrm{OFF}}y(I) \\ &= \left| \frac{(B+C)(mce^{-\sigma_c^2 f^2/2}\cos(fx) - mce^{-\sigma_s^2 f^2/2}\cos(fx))}{A + 2m + mce^{-\sigma_c^2 f^2/2}\cos(fx) + mce^{-\sigma_s^2 f^2/2}\cos(fx)} \right|, \end{aligned}$$

i.e

$$^{ON}y(I)+{}^{OFF}y(I)=\left|\frac{(B+C)(e^{-\sigma_c^2 f^2/2}-e^{-\sigma_s^2 f^2/2})\cos(fx)}{\frac{A+2m}{mc}+(e^{-\sigma_c^2 f^2/2}+e^{-\sigma_s^2 f^2/2})\cos(fx)}\right|. \tag{B.5}$$

To continue with our evaluation of the right-hand side of Eq. (B.3), we note that Eq. (B.5) implies that $^{ON}y(I)+{}^{OFF}y(I)$ varies only in the x direction. Therefore, we can apply Lemma 7 to the first convolution in Eq. (3):

$$O_\varepsilon(I)=({}^{ON}y(I)+{}^{OFF}y(I))\otimes\frac{1}{\sqrt{2\pi\sigma_\varepsilon^2}}e^{-x^2/2\sigma_\varepsilon^2}\otimes\lambda_\varepsilon(x,y),$$

where $\sigma_\varepsilon^2=\sigma_e^2\cos^2\varepsilon+\sigma_s^2\sin^2\varepsilon$. We can now apply Lemma 7 to the second convolution too:

$$O_\varepsilon(I)=({}^{ON}y(I)+{}^{OFF}y(I))\otimes\frac{1}{\sqrt{2\pi\sigma_\varepsilon^2}}e^{-x^2/2\sigma_\varepsilon^2}\otimes\frac{1}{\sqrt{2\pi\sigma_\varepsilon^2}}e^{-x^2/2\sigma_\varepsilon^2},$$

Applying Lemma 8 to the second convolution:

$$O_\varepsilon(I)=({}^{ON}y(I)+{}^{OFF}y(I))\otimes\frac{1}{\sqrt{4\pi(\sigma_e^2\cos^2\varepsilon+\sigma_s^2\sin^2\varepsilon)}}\times e^{-x^2/4(\sigma_e^2\cos^2\varepsilon+\sigma_s^2\sin^2\varepsilon)},$$

Combining Eqs. (B.5) and (B.6), the theorem is proved.

Appendix C Proof of Theorem 3

Lemma 9. *If $\tilde f(x)/f(x)>0$ and $g(x)>0$ $\forall x$, then:*

$$\min_x\left(\frac{\tilde f(x)-f(x)}{f(x)}\right)\le\frac{|\tilde f(x)|\otimes g(x)-|f(x)|\otimes g(x)}{|f(x)|\otimes g(x)}\le\max_x\left(\frac{\tilde f(x)-f(x)}{f(x)}\right).$$

Proof. Suppose $\tilde f(x)/f(x)>0$ and $g(x)>0$ $\forall x$ and manipulate $|\tilde f(x)|\otimes g(x)$ thus:

$$|\tilde f(x)|\otimes g(x)=\left|\frac{\tilde f(x)}{f(x)}f(x)\right|\otimes g(x)=$$

$$\left(\frac{\tilde f(x)}{f(x)}|f(x)|\right)\otimes g(x)\ (\text{as }\tilde f(x)/f(x)>0\ \forall x)$$

$$=\int_{\Re}\left(\frac{\tilde f(u)}{f(u)}|f(u)|\right)g(x-u)\,du=\int_{\Re}\frac{\tilde f(u)}{f(u)}|f(u)|g(x-u)\,du.$$

So, as $g(x)>0$ $\forall x$,

$$|\tilde f(x)|\otimes g(x)\le\int_{\Re}\max_u\left(\frac{\tilde f(u)}{\tilde f(u)}\right)|f(u)|g(x-u)\,du \tag{C.1}$$

and

$$|\tilde f(x)|\otimes g(x)\ge\int_{\Re}\min_u\left(\frac{\tilde f(u)}{\tilde f(u)}\right)|f(u)|g(x-u)\,du. \tag{C.2}$$

Continuing from Eq. (C.1):

$$|\tilde f(x)|\otimes g(x)\le\max_u\left(\frac{\tilde f(u)}{\tilde f(u)}\right)\int_{\Re}|f(u)|g(x-u)\,du$$

$$\le\max_u\left(\frac{\tilde f(u)}{\tilde f(u)}\right)(|f(x)|\otimes g(x)),$$

$$\frac{|\tilde f(x)|\otimes g(x)}{|f(x)|\otimes g(x)}\le\max_u\left(\frac{\tilde f(u)}{\tilde f(u)}\right)$$

and subtracting a '1' from both sides of the inequality above,

$$\frac{|\tilde f(x)|\otimes g(x)-|f(x)|\otimes g(x)}{|f(x)|\otimes g(x)}\le\max_u\left(\frac{\tilde f(u)-f(u)}{f(u)}\right). \tag{C.3}$$

Continuing from Eq. (C.2) in the same way:

$$\frac{|\tilde f(x)|\otimes g(x)-|f(x)|\otimes g(x)}{|f(x)|\otimes g(x)}\ge\min_u\left(\frac{\tilde f(u)-f(u)}{f(u)}\right). \tag{C.4}$$

and Eqs. (C.3) and (C.4) prove the lemma.

Theorem 3. *Suppose the input to Neumann's model is a sinusoidal grating with mid-range luminance m, contrast c and spatial frequency $f/2\pi$:*

$I(x,y)=m(1+c\cos(fx))$.

Then the output from the model at each of its $2n$ orientations $\varepsilon=0,\ \pi/2n,\ldots,(n-1)-\pi/2n$, denoted $O_\varepsilon(x,y)$, can be approximated by:

$$\tilde O_\varepsilon(x,y)=(B+C)\left(\frac{mc}{A+2m}\right)(e^{-\sigma_c^2 f^2/2}+e^{-\sigma_s^2 f^2/2})|\cos(fx)|\otimes\left(\frac{1}{\sqrt{4\pi(\sigma_e^2\cos^2\varepsilon+\sigma_s^2\sin^2\varepsilon)}}e^{-x^2/4(\sigma_e^2\cos^2\varepsilon+\sigma_s^2\sin^2\varepsilon)}\right),$$

where A, B, C, σ_c and σ_s, (all positive) are the free parameters of the model and $\sigma_e>\sigma_s$. This approximation introduces an error $|(\tilde O(x,y)-O(x,y))/O(x,y)|$ of not more than

$$\left(\frac{mc}{A+2m}\right)(e^{-\sigma_c^2 f^2/2}+e^{-\sigma_s^2 f^2/2}).$$

Proof. Suppose we define:

$$f(x)=\frac{(B+C)(e^{-\sigma_c^2 f^2/2}-e^{-\sigma_s^2 f^2/2})\cos(fx)}{\frac{A+2m}{mc}+(e^{-\sigma_c^2 f^2/2}+e^{-\sigma_s^2 f^2/2})\cos(fx)},$$

$$\tilde f(x)=(B+C)\left(\frac{mc}{A+2m}\right)(e^{-\sigma_c^2 f^2/2}+e^{-\sigma_s^2 f^2/2})\text{ and}$$

$$g(x)=\frac{1}{\sqrt{4\pi(\sigma_e^2\cos^2\varepsilon+\sigma_s^2\sin^2\varepsilon)}}e^{-x^2/4(\sigma_e^2\cos^2\varepsilon+\sigma_s^2\sin^2\varepsilon)}$$

Then we have:

$$O(x,y)=|f(x)|\otimes g(x)\text{ and }\tilde O(x,y)=|\tilde f(x)|\otimes g(x)$$

$$(\text{as } A,\ B,\ C,\ \sigma_c,\ \sigma_s,\ f,\ c,\ m>0),$$

so

$$\frac{\tilde{O}(x,\ y)-O(x,\ y)}{O(x,\ y)}=\frac{|\tilde{f}(x)|\otimes g(x)-|f(x)|\otimes g(x)}{|f(x)|\otimes g(x)}. \tag{C.5}$$

Furthermore,

$$\frac{\tilde{f}(x)-f(x)}{f(x)}=\left(\frac{mc}{A+2m}\right)(e^{-\sigma_c^2f^2/2}+e^{-\sigma_s^2f^2/2})\cos(fx), \tag{C.6}$$

and so since

$$\frac{\tilde{f}(x)-f(x)}{f(x)}\geq -\left(\frac{mc}{A+2m}\right)(e^{-\sigma_c^2f^2/2}+e^{-\sigma_s^2f^2/2})\forall x$$

$$\geq -\left(\frac{mc}{A+2m}\right)2>-1\ (\text{as } A>0),$$

we also have

$$\frac{\tilde{f}(x)}{f(x)}>0\ \forall x. \tag{C.7}$$

Finally, we note that:

$$g(x)>0\ \forall x. \tag{C.8}$$

Using Eqs. (C.5), (C.6), (C.7) and (C.8), we can now apply Lemma 9:

$$-\frac{mc}{A+2m}(e^{-\sigma_c^2f^2/2}+e^{-\sigma_s^2f^2/2})\leq\frac{\tilde{O}(x,\ y)-O(x,\ y)}{O(x,\ y)}$$

$$\leq\frac{mc}{A+2m}(e^{-\sigma_c^2f^2/2}+e^{-\sigma_s^2f^2/2}),$$

and the theorem is proved.

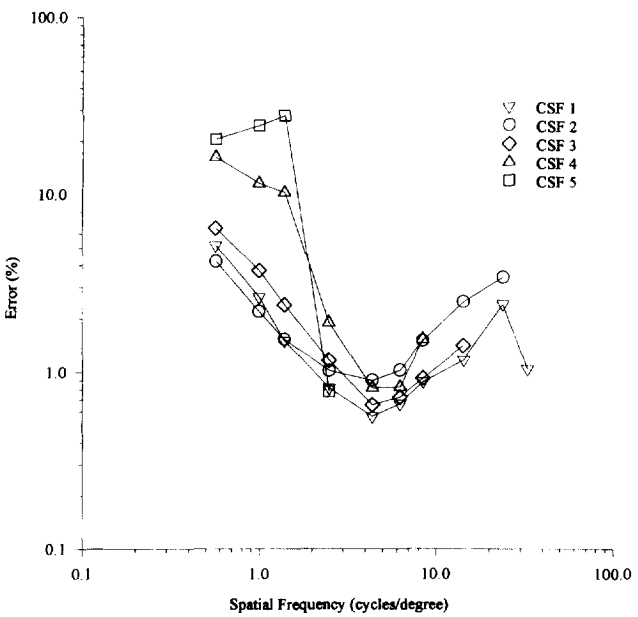

Fig. C.1. The worst possible error introduced when the approximation of Theorem 3 is applied to the CSF data.

Appendix C.1 Analysis of error

Helpfully, the error introduced by the approximation of Theorem 3 is not large when f, c, m, A, σ_c and σ_s, take values in the ranges of interest. Fig. C.1 shows it plotted at the spatial frequencies, contrasts and the five mid-range luminances of the CSF data of De Valois et al. [40], with the worst possible choice of model parameters A, σ_c and σ_s: A is set to a linear function of spatial frequency that is a lower bound of all the points plotted in Fig. 8, and σ_c and σ_s are made as small as possible (0.01° of visual angle) consistent with the estimated order of magnitude of their neurophysiological analogues (see Section 4.1.5). If the lowest three spatial frequencies are again neglected (see Section 4.3.4) then none of the five curves reaches a value of 3.5%. Furthermore, the error is less than 2.0% for spatial frequencies between 2.5 and 10.0 cycles/degree: a range encompassing the features of the data that was used for parametrization.

Corollary. To make a further simplification, consider only the vertically orientated output from the model, $\tilde{O}_{\pi/2}(x,\ y)$, which, from Theorem 3, can be approximated by:

$$\tilde{O}_{\pi/2}(x,\ y)=(B+C)\left(\frac{mc}{A+2m}\right)(e^{-\sigma_c^2f^2/2}+e^{-\sigma_s^2f^2/2})$$

$$\times|\cos(fx)|\otimes\left(\frac{1}{\sqrt{4\pi\sigma_s^2}}e^{-x^2/4\sigma_s^2}\right).$$

Although this formula is still very hard to manipulate mathematically, the surface it represents is qualitatively similar to a sinusoidal grating and approximate formulae for some of its properties can be found (e.g. Theorem 4, which is an approximate formula for the heights of its regular peaks).

Appendix D Proof of theorem 4

Lemma 10. *If $f\neq 0$:*

$$\max_x\left(|\cos(fx)|\otimes\frac{1}{\sqrt{2\pi\sigma^2}}e^{-x^2/2\sigma^2}\right)$$

$$=\max_x\left(|\cos(x)|\otimes\frac{1}{\sqrt{2\pi(\sigma f)^2}}e^{-x^2/2(\sigma f)^2}\right).$$

Proof. By the definition of convolution:

$$\max_x\left(|\cos(fx)|\otimes\frac{1}{\sqrt{2\pi\sigma^2}}e^{-x^2/2\sigma^2}\right)$$

$$=\max_x\left(\int_{\Re}|\cos(fu)|\frac{1}{\sqrt{2\pi\sigma^2}}e^{-(x-u)^2/2\sigma^2}\,du\right). \tag{D.1}$$

Making the substitution $u=u'/f(f\neq 0)$ in the integral on the right-hand side of Eq. (D.1) gives:

$$\max_x\left(\int_{\Re}|\cos(fu)|\frac{1}{\sqrt{2\pi\sigma^2}}e^{-(x-u)^2/2(\varepsilon)^2}\,du\right)$$

$$=\max_x\left(\int_{\Re}|\cos(u')|\frac{1}{\sqrt{2\pi\sigma^2}}e^{-(x-u'/f)^2/2\sigma^2}\frac{1}{f}\,du'\right)$$

$$=\max_x\left(\int_{\Re}|\cos(u')|\frac{1}{\sqrt{2\pi(\sigma f)^2}}e^{-(xf-u')^2/2(\sigma f)^2}\,du'\right)$$

$$=\max_x\left(\int_{\Re}|\cos(u')|\frac{1}{\sqrt{2\pi(\sigma f)^2}}e^{-(x-u')^2/2(\sigma f)^2}\,du'\right)$$

$$=\max_x\left(|\cos(u')|\otimes\frac{1}{\sqrt{2\pi(\sigma f)^2}}e^{-x^2/2(\sigma f)^2}\right)\text{ (by inspection).}$$

Theorem 4. If $\max_{x,y}(\tilde{O}_{\pi/2}(x,\,y))$ is approximated by:

$$\tilde{\tilde{O}}(f,\,c)=(B+C)\left(\frac{mc}{A+2m}\right)(e^{-\sigma_c^2f^2/2}-e^{-\sigma_s^2f^2/2})\times\left(\frac{2}{\pi}+\left(1-\frac{2}{\pi}\right)e^{-3.449(\sigma_sf)^{2.105}}\right)$$

then the error introduced, $|(\tilde{\tilde{O}}(f,\,c)-\max_{x,\,y}(\tilde{O}_{\pi/2}(x,\,y)))/\max_{x,\,y}(\tilde{O}_{\pi/2}(x,\,y))|$ may be written as a one-dimensional function of the product σ_sf (Eq. D.2.):

Proof. From Theorem 3:

$$\max_{x,y}(\tilde{O}_{\pi/2}(x,\,y))=\max_{x,\,y}\left((B+C)\left(\frac{mc}{A+2m}\right)\times(e^{-\sigma_c^2f^2/2}+e^{-\sigma_s^2f^2/2})|\cos(fx)|\otimes\left(\frac{1}{\sqrt{4\pi\sigma_s^2}}e^{-x^2/4\sigma_s^2}\right)\right)$$

$$=(B+C)\left(\frac{mc}{A+2m}\right)(e^{-\sigma_c^2f^2/2}+e^{-\sigma_s^2f^2/2})\times\max_x\left(|\cos(fx)|\otimes\left(\frac{1}{\sqrt{4\pi\sigma_s^2}}e^{-x^2/4\sigma_s^2}\right)\right).$$

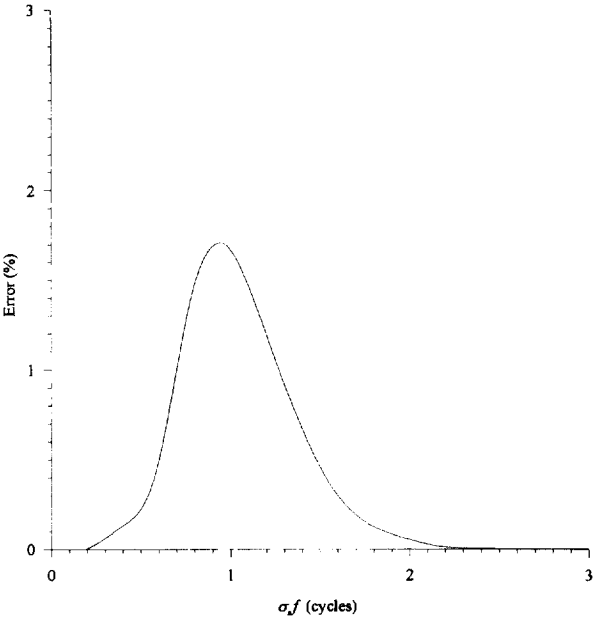

Fig. D.1. The error introduced when the approximation of Theorem 4 is applied.

So we can write the error $|(\tilde{\tilde{O}}(f,\,c)-\max_{x,y}(\tilde{O}_{\pi/2}(x,\,y)))/\max_{x,\,y}(\tilde{O}_{\pi/2}(x,\,y))|$ as Eq. D3:
From Lemma 10,

$$\max_x\left(|\cos(fx)|\otimes\frac{1}{\sqrt{4\pi\sigma_s^2}}e^{-x^2/4\sigma_s^2}\right)=\max_x\left(|\cos(fx)|\otimes\frac{1}{\sqrt{2\pi(\sqrt{2}\sigma_s)^2}}e^{-x^2/2(\sqrt{2}\sigma_s)^2}\right)=\max_x\left(|\cos(fx)|\otimes\frac{1}{\sqrt{4\pi(\sigma_sf)^2}}e^{-x^2/4(\sigma_sf)^2}\right).$$

Substituting this into Eq. (D.3) twice proves the theorem.

Appendix D.1 Analysis of Error

The error expression above has been evaluated computationally for a range of values of σ_sf: the graph of Fig. D.1 suggests that it stays below 2.0%.

$$\left|\frac{\left(\frac{2}{\pi}+\left(1-\frac{2}{\pi}\right)e^{-3.449(\sigma_sf)^{2.105}}\right)-\max_x\left(|\cos(x)|\otimes\frac{1}{\sqrt{4\pi(\sigma_sf)^2}}e^{-x^2/4(\sigma_sf)^2}\right)}{\max_x\left(|\cos(x)|\otimes\left(\frac{1}{\sqrt{4\pi(\sigma_sf)^2}}e^{-x^2/4(\sigma_sf)^2}\right)\right)}\right| \tag{D.2}$$

$$\left|\frac{\left(\frac{2}{\pi}+\left(1-\frac{2}{\pi}\right)e^{-3.449(\sigma_sf)^{2.105}}\right)-\max_x\left(|\cos(fx)|\otimes\frac{1}{\sqrt{4\pi\sigma_s^2}}e^{-x^2/4\sigma_s^2}\right)}{\max_x\left(|\cos(fx)|\otimes\left(\frac{1}{\sqrt{4\pi\sigma_s^2}}e^{-x^2/4\sigma_s^2}\right)\right)}\right| \tag{D.3}$$

Appendix D.2 Summary

The corollary to Theorem 3 stated that $O_{\pi/2}(x, y)$ can be approximated by $\tilde{O}_{\pi/2}(x, y)$ introducing an error of less than 2.0%–3.5%. In addition, the analysis above has shown that $\max_{x,y}(\tilde{O}_{\pi/2}(x, y))$ can be approximated by $\tilde{\tilde{O}}(f, c)$, introducing a further error of less than 2.0%. Therefore,

$$\max_{x,y}(O_{\pi/2}(x, y)) \approx (B+C)\left(\frac{mc}{A+2m}\right)(e^{-\sigma_i^2 f^2/2} - e^{-\sigma_c^2 f^2/2}) \times \left(\frac{2}{\pi} + \left(1 - \frac{2}{\pi}\right)e^{-3.449(\sigma_c f)^{2.105}}\right).$$

It can be shown that the error introduced by this approximation is typically less than 2%, although in exceptional circumstances can be as high as 6%.

References

[1] G.W. Humphreys, Psychophysical analyses of contour processing in humans: the case for qualitative tests, Image and Vision Computing 16(6–7) (1998) 501–511.

[2] H. Neumann, An Outline of a Neural Architecture for Unified Visual Contrast and Brightness Perception, Technical Report CAS/CNS-94-003, Boston University Center for Adaptive Systems and Department of Cognitive and Neural Systems, Boston, MA, 1994.

[3] S. Grossberg, E. Mingolla, Neural dynamics of perceptual grouping: textures, boundaries, and emergent segmentations, Perception Psychophys. 38 (2) (1985) 141–171.

[4] S. Grossberg, E. Mingolla, Neural dynamics of form perception: boundary completion, illusory figures, and neon color spreading, Psychol. Rev. 92 (2) (1985) 173–211.

[5] D. Marr. E. Hildreth, Theory of edge detection, Proc. Royal Soc. Lond. B 207 (1980) 187–217.

[6] L. Pessoa, E. Mingolla, H. Neumann, A contrast- and luminance-driven multiscale network model of brightness perception, Vision Res. 35 (15) (1995) 2201–2223.

[7] M.E.J. Raijmakers, H.L.J. van der Maas, P.C.M. Molenaar, Numerical bifurcation analysis of distance-dependent on-center off-surround shunting neural networks, Biol. Cybernetics 75 (6) (1996) 495–507.

[8] R.M. Haralick, Computer vision theory: the lack of thereof, Comput. Vision, Graphics Image Processing 36 (1986) 372–386.

[9] K. Price, Anything you can do, I can do better (no you can't)..., Comp. Vision, Graphics Image Processing 36 (1986) 387–391.

[10] R.M. Haralick, Methodology for experimental computer vision, in: Proc 1989 IEEE Computer Society Conference on Computer Vision and Pattern Recognition, San Diego, 1989, pp. 437–438.

[11] R.M. Haralick, Performance characterization in computer vision (Dialogue), CVGIP: Image Understanding 60 (1994) 245–249.

[12] J. Weng, T.S. Huang, Performance of computer vision algorithms, CVGIP: Image Understanding 60 (1994) 253–256.

[13] P. Meer, Computer vision: the goal and the means, CVGIP: Image Understanding 60 (1994) 257–259.

[14] R.M. Haralick, Comments on performance characterization replies, CVGIP: Image Understanding 60 (1994) 264–265.

[15] L. Ljung, System Identification: Theory for the User: Prentice Hall, Englewood Cliffs, NJ, 1987.

[16] H. Neumann, Mechanisms of neural architecture for visual contrast and brightness perception, Neural Networks 9 (6) (1996) 921–936.

[17] R.J. Watt, M.J. Morgan, A theory of the primitive spatial code in human vision, Vision Res. 25 (11) (1985) 1661–1674.

[18] R.J. Watt, Visual Processing: Computational, Psychophysical and Cognitive Research, Erlbaum, Hove, 1988.

[19] S. Grossberg, L. Wyse, A neural network architecture for figure-ground separation of connected scenic figures, Neural Networks 4 (1991) 723–742.

[20] M.A. Cohen, S. Grossberg, Neural dynamics of brightness perception: features, boundaries, diffusion and resonance, Perception Psychophys. 36 (5) (1984) 428–456.

[21] J. Malik, P. Perona, Finding boundaries in images, in: H. Wechsler (Ed.), Neural Networks for Perception, Vol. 1: Human and Machine Perception, Academic Press, London, 1992, pp. 315–344.

[22] A. Gove, S. Grossberg, E. Mingolla, Brightness perception, illusory contours, and corticogeniculate feedback, Visual Neurosci. 12 (1995) 1027–1052.

[23] A. Dobbins, S.W. Zucker, M.S. Cynader, Endstopped neurons in the visual cortex as a substrate for calculating curvature, Nature 329 (1987) 438–441.

[24] F. Heitger, L. Rosenthaler, R. von der Heydt, E. Peterhans, O. Kübler, Simulation of Neural Contour Mechanisms: Representing Anomalous Contours (to be published).

[25] R. von der Heydt, E. Peterhans, Mechanisms of contour perception in monkey visual cortex 1: Lines of pattern discontinuity, J. Neurosci. 9 (5) (1989) 1731–1748.

[26] J.F. Gerrissen, On the network-based emulation of human visual search, Neural Networks 4 (1991) 543–564.

[27] A. Treisman, Features and objects in visual processing, Scientific Am. 255 (5) (1986) 106–115.

[28] J.A. Marshall, Adaptive perceptual pattern recognition by self-organising neural networks—context, uncertainty, multiplicity, and scale, Neural Networks 8 (3) (1985) 335–362.

[29] S. Westland, D.H. Foster, A line-target-detection model using horizontal-vertical filters, in: A. Gale, K. Carr (Eds.), Visual Search III, Taylor and Francis, London, 1993.

[30] J. Skrzypek, B. Ringer, Neural network models for illusory contour perception, in: Proceedings of the IEEE Computer Society Conference on Computer Vision and Pattern Recognition, 1992.

[31] S. Wagner, A comparison of two neural network models for the perception of illusory contours, M.Sc. thesis, School of Computer Science, The University of Birmingham, Birmingham, 1993.

[32] H.R. Wilson, J.R. Bergen, A four mechanism model for threshold spatial vision, Vision Res. 19 (1979) 19–32.

[33] L.A. Segel, Simplification and scaling, Appl. Studies Math. Rev. 14 (4) (1972) 547–571.

[34] J.L. Casti, Nonlinear System Theory, Academic Press, London, 1985.

[35] H. Neumann, Toward a computational architecture for unified visual contrast and brightness perception: 1. Theory and model, in: Proceedings of the World Conference on Neural Networks (WCNN '93), 1993, pp. (I) 84–91.

[36] A. Fiorentini, G. Baumgartner, S. Magnussen, P.H. Schiller, J.P. Thomas, The perception of brightness and darkness-relations to neuronal receptive fields, in: L. Spillmann, J.S. Werner (Eds.), Visual Perception—The Neurophysiological Foundations, Academic, San Diego, FL, pp. 129–161.

[37] S. Grossberg, How does the brain build a cognitive code?, Psychol. Rev. 87 (1980) 1–51.

[38] I.R. Billups, Parametrizing models of early vision, Ph.D. thesis, School of Computer Science, University of Birmingham, Birmingham, England, 1995.

[39] D.H. Hubel, Eye, Brain, and Vision, Scientific American Library, New York, 1988.

[40] R.L. De Valois, H. Morgan, D.M. Snodderly, Psychophysical studies of monkey vision III. Spatial luminance contrast sensitivity tests of macaque and human observers, Vision Res. 14 (1974) 75–81.

[41] R.L. De Valois, K.K. De Valois, Spatial Vision, Oxford University Press, Oxford, 1990.

[42] D.J. Tolhurst, J.A. Movshon, I.D. Thompson, The dependence of response amplitude and variance of cat visual cortical neurones on stimulus contrast, Exp. Brain Res. 41 (1981) 414–419.